STUDIES ON PRODUCTION OF BIOFUEL AND BIOCHEMICALS FROM POWERPLANT ALGAE

Thesis

Submitted by

Kaustav Nath

[Exam Roll No. M4BPE19010]

[Class Roll No. 001710303010]

[Reg. No. 140630 of 2017-2018]

Under the Guidance of **Prof. (Dr.) Ranjana Chowdhury**

In the partial fulfilment for the award of the degree of

MASTER OF BIOPROCESS ENGINEERING

DEPARTMENT OF CHEMICAL ENGINEERING

JADAVPUR UNIVERSITY

JADAVPUR, KOLKATA-700032

INDIA

May2019

Declaration of Originality and Compliance of Academic Ethics

I hereby declare that this thesis contains literature survey and original research work by the undersigned candidate, as part of his Master of Bioprocess Engineering studies during academic session 2017-2019. All information in this document have been obtained and presented in accordance with academic rules and ethical conduct.

I also declare that, as required by these rules and conduct, I have fully cited and referenced all material and results that are fully authentic to this work.

Name : **Kaustav Nath**

Examination Roll Number : **M4BPE19010**

Thesis Title: **STUDIES ON PRODUCTION OF BIOFUEL AND BIOCHEMICALS FROM POWERPLANT ALGAE**

Signature:

Date:

CERTIFICATE

This is to certify that the thesis entitled ***"Studies on production of biofuel and biochemicals from powerplant algae"*** *has been carried out by Kaustav Nath in partial fulfilment of the requirements for the degree of Master of Bioprocess Engineering from Jadavpur University, Kolkata is recorded as bona fide work that has been conducted under the supervision of Prof. (Dr.) Ranjana Chowdhury. The contents embodied in the thesis have not been submitted to any other university for the award of any degree or diploma.*

Prof. (Dr.) Debashis Roy
Head of Department and Professor
Chemical Engineering Department
Jadavpur University

Prof (Dr.) Ranjana Chowdhury
Project Supervisor, Professor& former Head
Chemical Engineering Department
Jadavpur University.

Prof. Chiranjeeb Bhattacharjee
Dean of Faculty and Engineering Technology
Jadavpur University.

Acknowledgement

I am privileged to take this opportunity in expressing my deep sense of gratitude towards my supervisor Prof. (Dr.) Ranjana Chowdhury, Professor and Former Head of the Department, Department of Chemical Engineering, Jadavpur University, Kolkata, India for her inspiring encouragement and valuable guidance throughout the work. She always bestowed parental care upon me and evinced keen interest in solving my problems. Her sober personality always inspired me to strive more and accomplish superior results. An erudite teacher, a magnificent person and a strict disciplinarian, I am really indebted and also feel endowed with her affection, thanks for her critical remarks and suggestions which enabled me to complete this work.

I am also grateful to Prof. (Dr.) Debashis Roy, Head of the Department of Chemical Engineering for providing me with all necessary facilities to carry out the work.

I would like to specially thank Ms Sumona Das, Mr. Dinabandhu Manna, Mr Shiladitya Gosh and Mrs. Jigeesha Panda for their sincere support and motivation without which this report would not have been materialized.

My thanks to technical and non-technical staffs of Department of Chemical engineering, Jadavpur University, for their help.

I would also like to thank to my batchmates for helping me every time when things went awry.

I am thankful to God almighty for bestowing me with good fortune, everywhere to show his presence.

Last but not the least I would like to thank my parents who have helped and guided me since childhood and are still willing to support me through my endeavours.

Kaustav Nath
Department of Chemical Engineering
Jadavpur University

Abstract

Microalgae have been studied for a long period of time for their ability to sequestrate CO_2 and metabolise lipid body and essential fatty acids. With rise in demand for renewable and environmentally friendly fuel, algae have been identified as a potential feedstock for biofuel production. Microalgae are also able to convert the biomolecules in substrate into useful biochemicals. In the present study investigations have been made to determine the growth and lipid kinetics parameters of algal strain *L. subtilis JUCHE1* in photoautotrophic and photoheterotrophic growth modes. It was noted that the highest biomass concentration and productivity were observed in photoautotrophic growth mode. The maximum specific growth rate was evaluated to be 3.667 day^{-1} for photoautotrophic mode which was much higher than 0.882615 day^{-1} obtained in photoheterotrophic mode. The values of K_S 0.24972 g/L and 0.01023 g/L for the respective mode of growth. Similarly, the values of K_I obtained for the respective growth modes were 0.007965 g/L and 0.1945 g/L. In case of lipid accumulation and productivity, the highest content was 56.345% for photoheterotrophic growth while only 12.5% for photoautotrophic mode which signifies that the strain shows oleaginous trait in photoheterotrophic mode of growth by sacrificing growth and biomass productivity. The maximum productivity, maximum specific rate of lipid formation, half saturation rate constant and inhibition constant obtained for photoheterotrophic batches were 0.062055 g/L/day, 0.15701 day^{-1}, $2.7x10^{-3}$ g/L and 0.73804 g/L respectively. The study also identified the that the algal oil extracted from the chosen strain contains essential fatty acids. Model simulation has been conducted for predicting fit of experimental and theoretical data obtained by solving the differential mass balance equations have been solved for the experiments conducted with CO_2 concentration of 15%. Furthermore, pigment extraction was undertaken in the current study that suggests that Dimethyl sulphoxide is a good solvent for extracting Chlorophyll a and b while Diethyl ether gives better results for carotenoid extraction.

Table of Contents

List of figures

List of tables

Chapter 1: Introduction

1.1 Comprehensive overview of global challenges

The development of renewable energy has been attracting scientific interest worldwide. The primary reason is the limited fossil fuel reserves. Petroleum and other such derivatives took millions of years to form and the reserves are slowly drying up. The long-term challenges that are needed to be addressed within the fossil fuel driven economy are namely climate change, economic development as well as energy security. The overwhelming urge to develop has compelled humans to over utilize conventional fuels like coal and petroleum as energy source. The increasing rate of industrialisation in the growing and emerging economies are primarily responsible for the increasing global demand of energy.

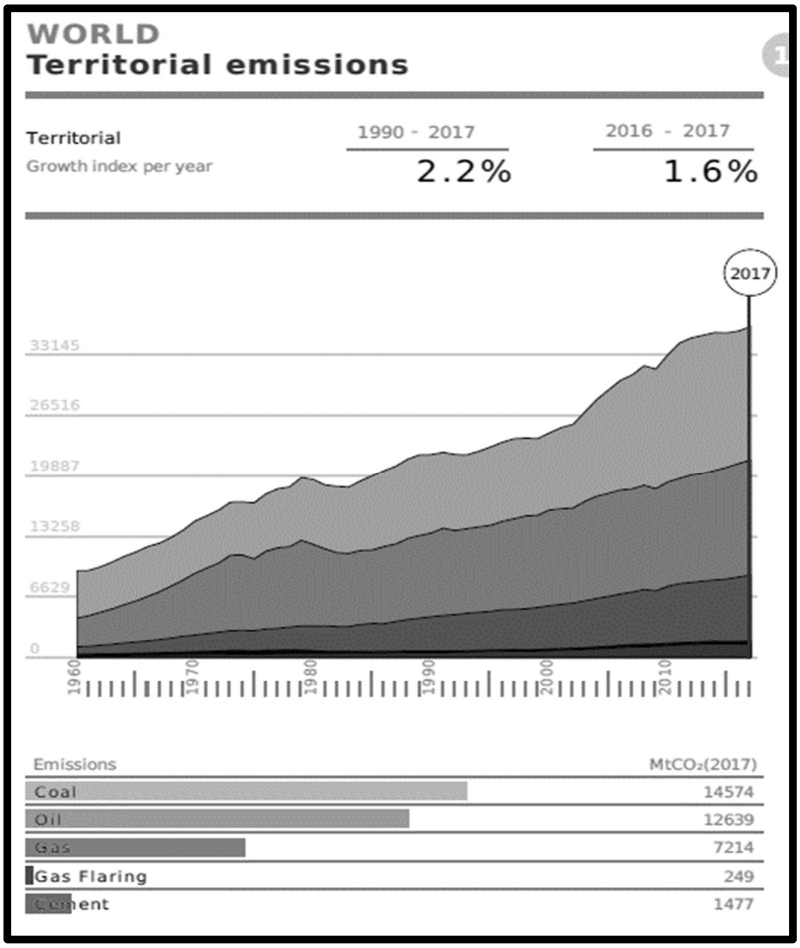

Figure 1: Global territorial CO_2 emissions

(Source: globalcarbonatlas.org, 2019**)**

This growing demand for fossil fuel derived energy has detrimental impacts on the environment and climate. The changes in the climate system have been reported to increase

due to the increasing use of fossil fuels which in turn emit greenhouse gases like CO_2 which is the primary by-product of fossil fuel combustion. The atmospheric CO_2 concentration has breached the 400-ppm mark as seen in Figure 2. Carbon emissions have kept on rising and average earth temperature has increased from 13.79℃ in 1919 to around 14.5℃ in 2018 (www.earth-policy.org/datacenter).

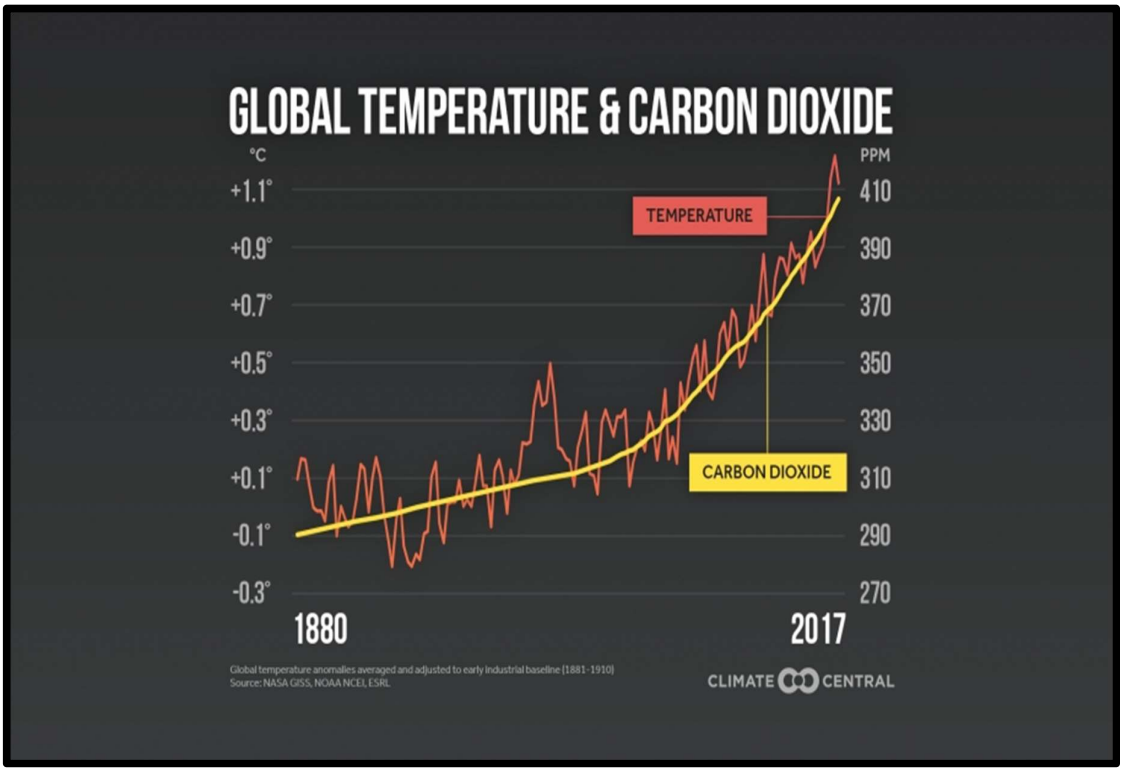

Figure 2: Increase in global temperature and CO_2 concentration

(Source: climatecentral.org, 2018**)**

The Intergovernmental Panel on Climate Change (IPCC) report has outlined that global warming is the greatest challenge to the present-day society, a claim which has been supported by other environmental reports as well (ipcc.ch, 2018). The increasing temperature is responsible for the changes in the climate system and also for the destabilisation of polar ice caps, thus endangering ecological balance. In order to moderate the harmful effects of global warming it is necessary to take immediate steps. The increasing influence of geopolitics and implementation of the stringent environmental policies for minimising the effects of greenhouse gases is also significantly responsible for the increased focus towards the greener alternatives.

Carbon-climate observations have revealed that the overall CO_2 uptake by the natural carbon sinks have increased significantly as clearly depicted in Figure 3. On an average, in the past

few decades the anthropogenic fossil fuel combustion is responsible for release of 10 gigatons of CO_2 per year (shrinkthatfootprint.com, 2013). The terrestrial and aquatic natural sinks uptake only a marginal amount of the released carbon. The majority of the released carbon dioxide remains in the atmosphere itself. Even with this knowledge, the dependence on fossil fuels has not decreased. If nothing else, the dependence has only increased. The increasing accumulation of the global emissions have resulted in focused approach to mitigation as well as sequestration efforts in order to maintain the carbon balance.

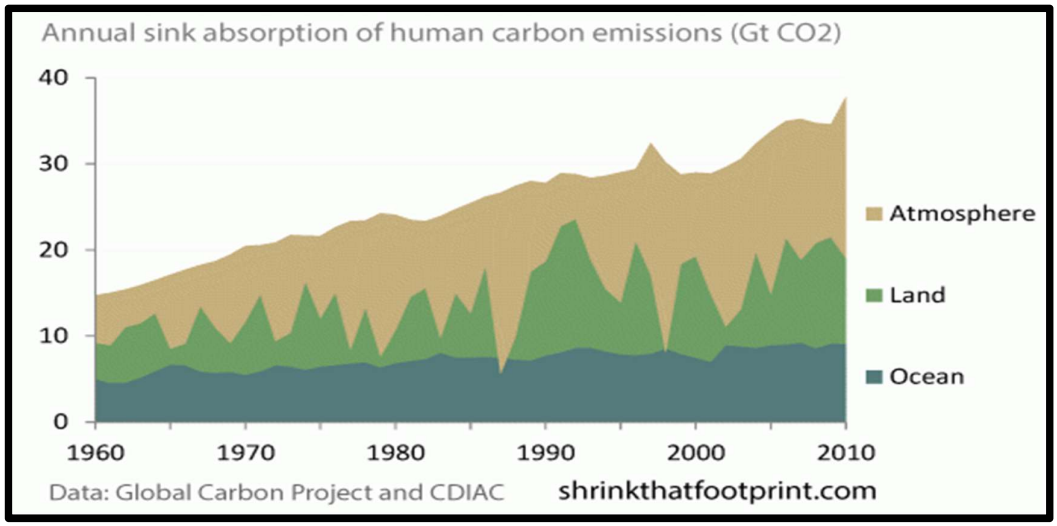

Figure 3: Annual absorption of CO_2 emissions by natural carbon sinks

(Source: shrinkthatfootprint.com, 2013**)**

As discussed earlier, fossil fuel combustion is directly related to the surface temperature on the polar ice caps. Human decadence pertaining to carbon emissions and inability of large corporations to identify and incorporate green processes in their operations has largely contributed to the increasing emissions of greenhouse gases. This has led the focus towards integrated bioremediation processes which offers a wide spectrum of end products such as hydrogen by the direct or indirect photolysis, biodiesel by transesterification, biomethane by anaerobic digestion, bio ethanol by fermentation, bio oil using thermochemical conversion as well as green diesel which involves direct catalytic hydrothermal liquefaction.

1.2 Concept of biorefineries and bioremediation

The concept of biorefinery and bioremediation can be considered as two faces of the same coin. The International Energy Agency Bioenergy Task 42 defines a biorefinery as "the means of sustainable processing of biomass into a spectrum of bio-based products (food, feed, chemicals, materials) and bioenergy (biofuels, power and/or heat)" (ieabioenergy.com, 2013).

By extrapolating the same concept, an algal biorefinery can be defined as a processing unit where algal biomass is processed fuel and wide spectrum of end products as seen in the figure below. Bioremediation can be explained as a process that can be used for treating contaminated soil or water due to alteration of the environmental conditions which in turn stimulates microbial growth that degrades the targeted pollutants (Chen *et a*l. 2012).

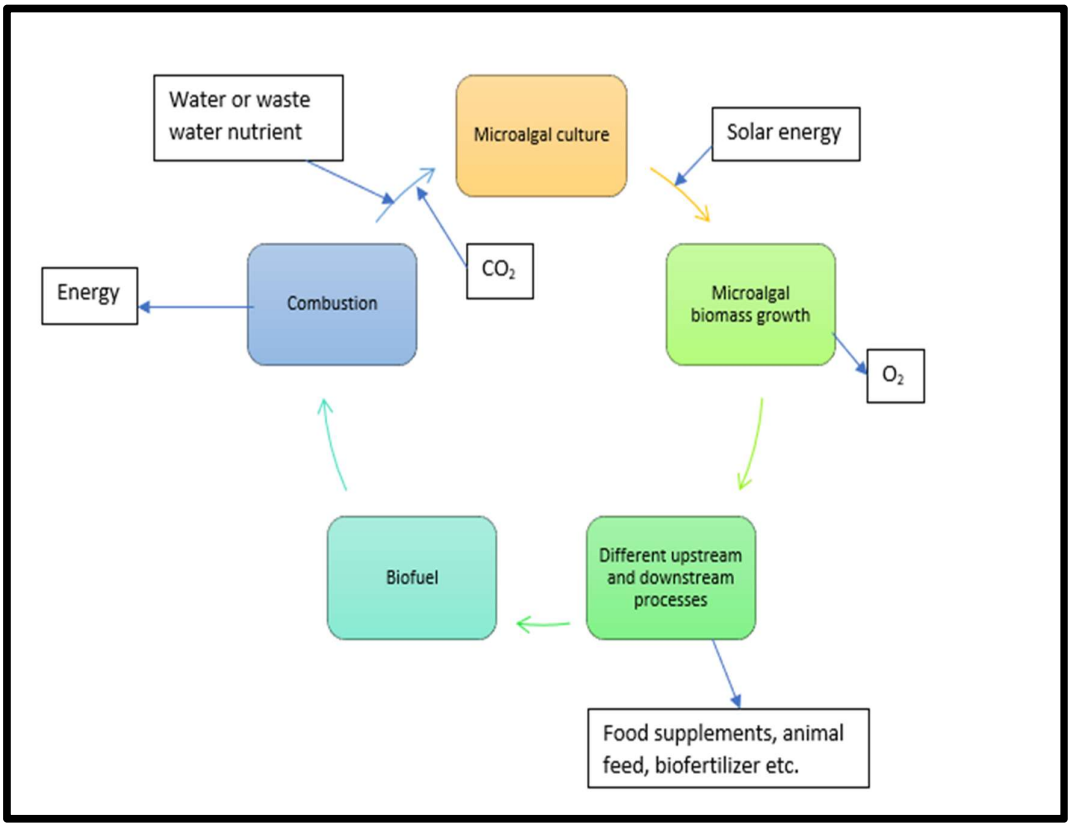

Figure 4: Different uses of microalgae as feedstock

1.3 Evolution of biofuels

Extensive research has been done in development of biofuels from different feedstocks. The first generation of biofuels included food crops as primary substrate for production of biofuel, however, this resulted in a food-fuel conflict and thus, the first generation of biofuels were not pursued in the long run. Ethanol is a very good example of first-generation biofuel. The second generation of biofuels were derived by the action of microorganisms on carbonaceous wastes such as lignose or cellulose. Biogas is a type of second-generation biofuel. The third generation of biofuels mainly constitutes of biofuel derived from algal biomass (Drapcho *et al.* 2008).

1.4 Algae as biodiesel feedstock

Algae can be highly effective in context of ecological sustainability as well as economic relief in industries when they are used as bioremediation agents for removal of the inorganic nutrients that may be present in wastewater for improving the quality of water. Investigations that have been carried out to determine the most suitable means of deriving the green alternatives have identified algal biomass as a potential source of biofuel due to two primary reasons:

1. The ability of algal biomass to make use of atmospheric CO_2 as substrate in presence of sunlight.
2. The ability of algal biomass to convert the sequestrated CO_2 into intracellular lipid bodies that can be collected and converted into biofuel.

Algae are microscopic or macroscopic organisms that can be found suspended in water and their biological activities are driven by the energy from photosynthesis. Their characteristics are very similar to that of the terrestrial plants. The class of algae basically comprises of cyanobacteria (bacteria with chlorophyll pigment), diatoms, unicellular plants as well as protists. One of the primary differences of microalgae from higher as well as terrestrial plants is the non-requirement of the vascular system that is utilised by the higher plants for nutrient transfer (Deng *et al.*2009). A large variety of algal species are available in nature that can survive in a number of environments ranging from fresh water to highly saline sea water.

Algae are predominantly photoautotrophs which utilise sunlight to utilise the available CO_2 for their metabolic activity. They can also fixate carbon dioxide in water by turning them into organic compounds such as the bicarbonate salts without formation of any other secondary pollutants. As reported by Bermudez *et al.* (2015), the microalgae apart from being used as biofuel can be also used for obtaining a wide variety of end products such as essential fatty acids like Docosahexaenoic Acid (DHA), Eicosapentaenoic Acid (EPA), α-Linoleic Acid (ALA) to name a few. It can be also utilised as animal feed and chemical feedstock as well. Microalgae are also capable of high photosynthesis rates which consequently means a rapid growth rate.

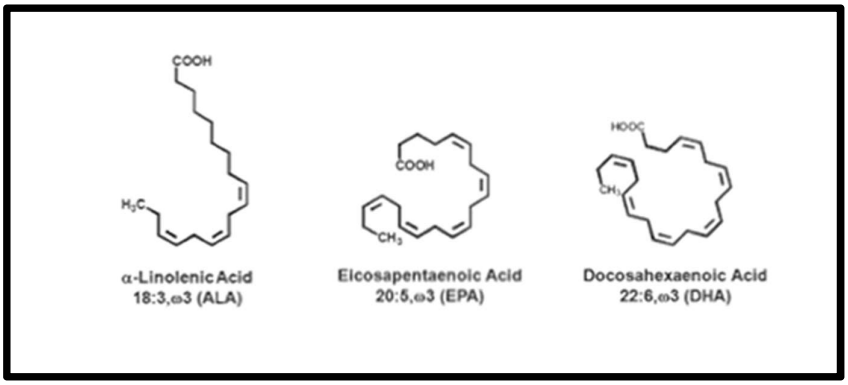

Figure 5: Essential fatty acids (ω-3 fatty acids) that can be extracted from microalgae

(Source: lpi.oregonstate.edu, 2019**)**

These organisms are highly adaptable and the overall cost of operation is low. The carbon fixation depends primarily on organism species, cultivation conditions, concentration of CO_2 and presence of other toxic contaminants in case of flue gas. Some algal species also exhibit heterotrophic growth and investigations have been carried out to determine the impact of such growth conditions on the growth kinetics as well as lipid content in algae (Khanra *et al.* 2017).

Chapter 2: Aim and objectives

2.1 Aim

The aim of the study is to investigate the effect of heterotrophic and autotrophic growth conditions on the growth kinetics as well as the lipid content of algal species *Leptolyngbya subtilis JUCHE1* (LS) by conducting batch study experiments small scale algal bioreactors. The CO_2 sequestration potential of the isolated algal strain is also a photoheterotrophic parameter that will be analysed in the course of the experiment. The harvested biomass will be subsequently utilised for pigment and lipid extraction which will later be characterised using Spectrophotometer and GC-MS respectively.

2.2 Objectives

- To investigate the algal growth and lipid kinetics in photoautotrophic mode
- To investigate the algal growth and lipid kinetics in photoheterotrophic mode
- To compare the pigment extraction using different extraction solvents
- To compare the growth and lipid kinetics parameters in photoautotrophic and photoheterotrophic mode
- To determine the presence of essential fatty acids using GC-MS
- To develop mathematical modelling equations for the batch mode experiment and validation of the same for gas phase CO_2 concentration of 15%

Chapter 3: Literature review

Author name and year of publication	Strain	Key findings
Kong *et al.* 2013	*Chlorella vulgaris*	The feasibility of biodiesel derived glycerol as potential algal substrate has been discussed. The objective of the study was to investigate the ability of microalgae to utilise complex carbon substrate for production of algal biomass as well as the biochemical components like pigments, lipids, carbohydrates and proteins. The article also highlights ability of the selected strain to utilise glycerol as the sole exogenous source of carbon. The organism was grown on modified soil extract medium (SEM) having a pH of 7.2 at 30°C for a total of 96 hours of incubation time. Glycerol concentration of 1 to 10 g/L and glucose concentration of 2 g/L were taken as substrate concentration in this study. The working volume for the study was 100 ml and cultures were grown under 12-hour dark:12-hour light period having light intensity of 2.5 kLux. The study concludes that Chlorella vulgaris is able to utilise glycerol as sole source of exogenous carbon. However, when the organism was grown in mixture of glucose and glycerol, there was a significant improvement in growth, lipid contents, biomass yield and productivity. Maximum biomass concentration, growth rate, productivity and lipid content were 2.16 g/L, 0.94 day^{-1}, 0.539 g/L/day and 9.5% respectively for 10 g/L glycerol

Perez-Garcia *et al.* 2011	NA	This review article primarily focuses on the ability of microalgae to grow in heterotrophic medium by utilising exogenous carbon substrate in absence of light. Since photoautotrophic requires use of complicated processes and is expensive, heterotrophy has become a niche of microalgal cultivation process. The article identifies the key issues of heterotrophic growth and also sheds light on metabolism of different carbon substrates like glucose, glycerol, waste water and acetate. Apart from metabolism of carbon, the review article also discusses nitrogen metabolism followed by investigation of the effect of different substrate metabolism pathways that impacts the yield of lipids, Polyunsaturated Fatty Acids (PUFA), biodiesel as well as pigments.
Lin *et al.* 2012	*Dunaliella tertiolecta*	The current work reports the inability of marine species like *Dunaliella tertiolecta* to regulate cell volume in response to osmotic shock. Their study revealed that the species was able to uptake exogenous glycerol in short amount of time. However, the is article only able to justify glycerol uptake by membrane bound glycerol uptake proteins as a an osmoregulatory in response to high salt stress conditions
Amritpreet *et al.* 2016	NA	In this review article the several favourable stress factors have been identified that can be useful inducing microalgal lipid and carotenoid production. The study tries to analyse the ability of microalgae to utilise glycerol as carbon source

		in heterotrophic or mixotrophic growth conditions. It reveals that in higher glycerol concentrations the stress increases the lipid productivity in mixotrophic condition with lower glucose concentrations
Aubert *et al.* 1994	NA	The presented work tries to investigate effects of glycerol on metabolism in higher plants like sycamore. According to the article the breakdown of glycerol in higher plants can be explained by enzymes present in cytoplasm. In lower external glycerol concentrations, the scavenging power of the enzyme glycerol kinase is considerably increased. The intracellular glycerol 3 phosphate derived by phosphorylation of glycerol is channeled to glycolytic pathway assisted by the cytosolic or plastid NAD-linked glycerol phosphate dehydrogenase.
Khanra *et al.* 2017	*Euglena gracilis*	The study reports the effect of crude glycerol on lipid enhancement and FAME characterisation in *Euglena gracilis.* The strain shows excellent growth as well as lipid synthesis potential under mixotrophic conditions in presence of organic carbon. The study reported highest biomass concentration of 2.63 g/L and a lipid content of 27.64% The study also positively reported the effect of biodiesel derived glycerol on lipid accumulation (49.46%) and 93.45% of FAMES consisting appropriate quantities of saturated as well as unsaturated C16-C18 fatty acids. The highest biomass and lipid concentration observed for crude glycerol were 3.18 g/L and 1.573 g/L

		respectively
Robaina *et al.* 2007	*Grateloupia doryphora*	The present work tries to investigate the heterotrophic activity of red macroalgae in glycerol assisted medium under illumination. The findings of the study suggest that if glycerol or glycerol derived organic carbon metabolism begins with photophosphorylation, the extra ATP derived from photosynthetic light dependent reactions would be utilised for metabolising the net influx of glycerol. They also conclude that the light activated glycerol respiration is not dependent on the supply of photosynthetic ATP to glycerol metabolism pathways.
Man & Chen, 2000	*Spirulina platensis*	The effect of cyanobacteria cells light in response of mixotrophic growth has been investigated in the current article. Their study revealed that in comparison to photoautotrophic growth where the growth is sensitive to light conditions, the mixotrophic cultures had a fast growth rate and higher biomass concentration. The study also reported decline in light dependent oxygen evolution as well as efficiency of photosystem II in photoautotrophic batches when exposed to high density of photon flux i.e. 3000 μmol/m^2/s.
Ren *et al.* 2017	*Chlorella vulgaris*	The current study tries to improve nutrient from real wastewater as well as enhance biomass productivity. The organism was cultivated in a pilot scale photobioreactor having an optimal crude glycerol concentration of 1 g/L. The study

		yielded a maximum biomass productivity of 460 mg/L/day and a lipid content of 27%.
Leite *et al.* 2014	*Chlorella sp*	The current paper discusses the use of glycerol and xylose for boosting lipid yield. The investigations were carried on indigenous microalgae, mainly *Chlorella sp*., sourced from Université de Montréal collection of microalgae. The work reports high specific growth rates of 1.52 day^{-1} in glycerol assisted growth. It was also noted that addition of glycerol in culture medium did not translate to increased biomass productivity, but it was observed that in eight of the ten strains investigated, the lipid production was high when cultivated in heterotrophic conditions.
Chen *et al.* 1996	*Spirulina platensis*	The current paper investigates the growth as well as phycocyanin formation in microalgae under photoheterotrophic culture conditions. The investigation reported highest specific growth rate of 0.62 day^{-1}, biomass concentration of 2.66 g/L and phycocyanin production of 322 mg/L in glucose assisted growth. In acetate assisted growth the maximum biomass concentration was 1.81 g/L, phycocyanin production of 246 mg/L and highest biomass concentration of 1.81 g/L. The optimum glucose concentration was found to be 2.5 g/L where in the growth rate increased with increase in light intensity. Photoinhibition occur beyond 4 kLux. The article also noted that phycocyanin formation was favoured in presence of light. Decrease in light intensity to 2 kLux or

		less shifted optimal glucose concentration from 2.5g/L to 5 g/L.
Rajaram *et al.* 2018	*Amphora coffeaeformis RR03*	The results showed increased growth of the newly identified marine diatom *A. coffeaeformis RR03* on 21st day with CO_2 supply. Oil production by the strain was around 36.19 megajoule. *A. coffeaeformis RR03* accommodated 47.72% 16-octadecanoic acid methyl ester and 19.58% pentadecanoic acid, 13-methyl, and methyl ester that is required for production of quality biofuel.
Ruangsomboon *et al.* 2017	*Botryococcus braunii KMITL 2*	In this study, at 5% CO_2 the algal strain had the highest yield of hydrocarbons. At 10% biomass yield was 2.7 times that of control. It was also speculated that high concentration of CO_2 may be helpful in long term stability when storing biodiesel.
Huang & Su, 2014	*Chlorella vulgaris*	Growth conditions like pH, carbon dioxide in media and light intensity were manipulated in the present study to obtain a high lipid content as well as productivity. The optimum growth condition reported in the article is neutral pH, 2.9 kLux and an elevated CO_2 concentration of 30%. The maximum biomass concentration obtained at this concentration was 1.13 g/L. The organism also showed appreciable tolerance in 50% CO_2 concentration achieving a biomass concentration of 1.083 g/L. Maximum biomass productivity obtained in the study was 3.25 day^{-1}. The investigation also chronicles a lipid content of 45.68% and lipid productivity if 86.03 mg/L/day

		making the organism a potential biofuel feedstock under high CO_2 concentrations.
Wang *et al.* 2018	*Graesiella sp.WBG1*	The reported work discusses the use of exogenous CO_2 from flue gas for regulating pH in large scale microalgal cultivation combining bio fixation of CO_2 and biodiesel production. The organism was studied under different pH levels regulated by 15% exogenous CO_2 in open raceway reactors. CO_2 fixation was most optimum at pH 8-9. The highest fixation rate, lipid content and lipid productivities obtained were 0.26 g/L/day, 46.28% and 64.8 mg/L/day.
de Morais *et al.* 2007	*Spirulina sp.* and *Scenedesmus obliquus*	The current report tries to underline the contribution of microalgae and cyanobacteria as bio sequestrator of atmospheric CO_2. The culture period for both the strains was 5 days after which cell death occurs. the maximum specific growth rate as well as the maximum productivity was obtained for Spirulina sp. i.e. 0.44 day^{-1}, 0.22 g/L/day, both with 6% (v/v) carbon dioxide. The maximum biomass concentration obtained was 3.50 g L−1 in cultures having 12% (v/v) carbon dioxide. The maximum rate of daily CO_2 bio fixation was found to be 53.29% in case of 6% (v/v) CO_2 concentration and 45.61% for 12% CO_2. However, in case of S. obliquus the rate of bio fixation was 28.08% and 13.56% for 6% (v/v) and 12% (v/v) CO_2 concentration.
Pegallapati & Nirmalakhandan, 2013	*Scenedesmus sp.* and *Nannochloropsis*	The presented work discusses the growth of the algal strains *Scenedesmus sp.* and *Nannochloropsis salina* in photobioreactor

	salina	having artificial light and varying CO_0-air (vol/vol) ratios. A constant rate of 0.8 L/min air supply was maintained corresponding to the gas to culture volume ratio of 0.044 min^{-1}. The CO_2-air ratios of 4% and 1% were noted to be the optimal substrate concentration for both *Scenedesmus sp.* and *N. salina*. The article also reports volumetric productivities of 0.40 g/L/day and 0.104 g/L/day respectively. Under the continuous mode of operation complemented by regular harvesting at the optimal CO_2-air ratios the maximum constant biomass concentration obtained was 1.40 g/L and 0.52 g/L respectively. The average biomass productions reported for the two species were 2.53 and 0.93 g/day respectively.
de Morais *et al.* 2007	*Scenedesmus obliquus* and *Chlorella kessleri*	The study tries to detail the isolation as well as selection of the algal strains *Scenedesmus obliquus* and *Chlorella kessleri* from Presidente Medici coal fired thermoelectric power plant waste treatment ponds for investigating the growth characteristics of the organisms when they were subjected to different CO_2 concentrations. In 6% and 12% CO_2 concentrations, the strain *C. kessleri* reported a high maximum specific growth rate of 0.267 day^{-1}. The maximum biomass productivity of 0.087 g/L/day was obtained for 6% CO_2. In case of *S. obliquus*, the maximum biomass concentration was 1.14 g/L at 12% CO_2. The study also reported both the algal strains showed positive results when the grown in culture medium

		containing 18% CO_2, which suggests that these algal strains can be used for bio fixation of CO_2 emitted from the thermoelectric power plants
Shih-Hsin Ho *et al.* 2012	*Scenedesmus obliquus CNW-N*	The optimal range of parameters like CO_2 concentration, magnesium concentration, CO_2 flow rate and light intensity in the present study for achieving the best performance in terms of specific growth rate as well as CO_2 fixation rate were found out to be 2.0–2.5%, 1.7–2.7 mM, 0.3–0.5 vvm and 180–250 μmol/m^2/s, respectively. Maintaining these optimal parameters helped in achieving a specific growth rate and CO_2 fixation rate greater than 1.22 day^{-1} and 800 mg/L/day. The study also made use of the semi-batch operations which actually enhanced the biomass productivity, CO_2 fixation rate as well as photosynthesis efficiency to 1030 mg/L/day, 1782 mg/L/day and 10.5% respectively.

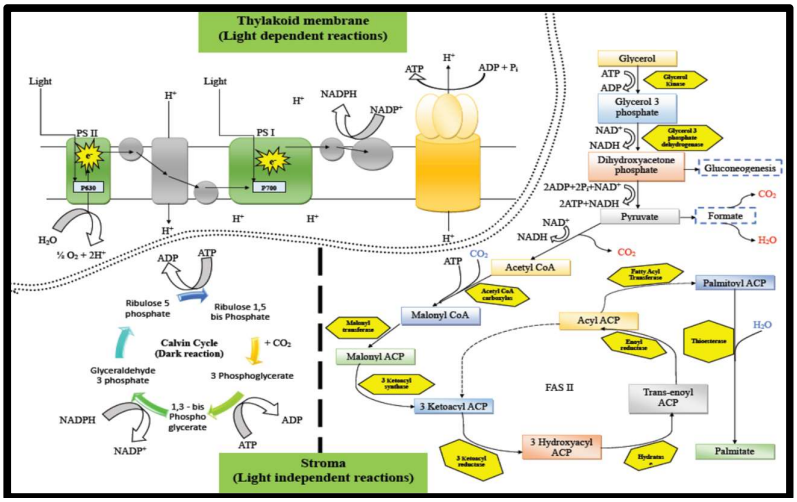

Figure 6: Brief overview of metabolic pathways for utilisation of different carbon source and fatty acid synthesis in microalgae

(Source: Nelson *et al.* 2008)

Chapter 4: Theoretical analysis

By making mass balance for CO_2 in liquid phase, biomass and lipid in the batch reactor over a time interval 'Δt' with $\Delta t \to 0$, the following equations have been obtained:

For CO_{2L}:

$$\frac{dCO_{2_L}}{dt} = -\frac{1}{Y_{X/S}} . \frac{\mu_{\max} C_{CO_{2_L}}}{K_{S_{CO_2}} + C_{CO_{2_L}}} . C_X \qquad (1)$$

For Biomass:

$$\frac{dC_X}{dt} = \frac{\mu_{\max} C_{CO_{2_L}}}{K_{S_{CO_2}} + C_{CO_{2_L}}} . C_X \qquad (2)$$

For Lipid:

$$\frac{dC_L}{dt} = \frac{q_{p\max} C_{CO_2 L}}{K_{P_{CO_2}} + C_{CO_2 L}} . C_X \qquad (3)$$

The differential mass balance equations have been solved for the experiments conducted with CO_2 concentration of 15% using ODE45 in MATLAB with the following boundary conditions:

At $t = 0$

$C_{CO_2,L} = C_{CO_2 L},0$

$C_X = C_X,0$

$C_L = C_L,0$

The initial values are as follows:

$C_{CO_2 L},0 = 0.1637 g/l$

$C_X,0 = 0.2473 g/l$

$C_L,0 = 0.01 g/l$

MATLAB function

```
%  Function file:

function dydt = LS(t, y)
A=1.58207;
umax=3.667;
Ks=0.91565;
qpmax=0.15289;
Kp=0.1808;
dydt = zeros(3,1);
%A=3.6422*(t^2)-12.509*t+17.265;
dydt(1) = -(1/A)*(umax*y(1)*y(2))/(Ks+y(1));
dydt(2) = (umax*y(1)*y(2))/(Ks+y(1));
dydt(3) = (qpmax*y(1)*y(2))/(Kp+y(1));
end


% script file:

tspan = [0: 1: 4];
Y0 = [0.16368  0.2473 0.01];
[T, Y] = ode45(@(t, Y) LS(t, Y), tspan, Y0);
[T Y]
plot(T,Y)
```

Chapter 5: Materials and methods

5.1 Equipments and apparatus used

- Digital weighing machine (Sartorius)
- Autoclave
- Hot air oven
- B. O. D. incubator fitted with 4 CFL light
- Table Top Centrifuge (Spinwin, India)
- Laminar air flow bench
- Gas Chromatography-Mass Spectrometry (Perkin Elmer, USA)
- Spectrophotometer (Perkin Elmer, USA)
- Light field microscope
- Orsat apparatus

5.2 Algal strain and media preparation

The algal strain *Leptolyngbya subitilis JUCHE1* used in the current study has been isolated from water bodies in and around coal-fired thermal power plants in Sagardighi, Berhampur, West Bengal. It can be clearly observed in Figure 7, that under the microscope the microalgae specimen has a thread like morphology.

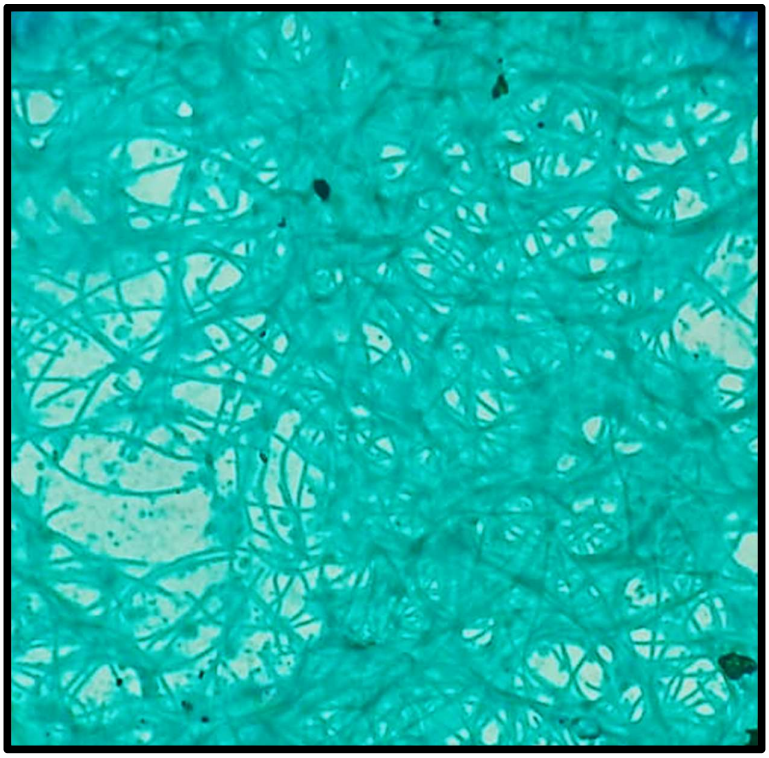

Figure 7: The algal strain L. subtilis JUCHE1 under light field microscope

Modified 18 medium was used as the minimal salt medium in the current work. For a basis of 1 litre, the composition of the media is as follows:

Major salts

- 1.5g $NaNO_3$
- 0.38g $MgSO_4.7H_2O$
- 0.12g K_2HPO_4
- 0.11g $CaCl_2.2H_2O$

Minor salts

- 0.07g NaCl
- 0.01g $Fe_2(SO_4)_3.4H_2O$
- 0.003g H_3BO_3, 0.002g $MnSO_4.4H_2O$
- 0.0003g $ZnSO_4.7H_2O$
- 0.00008g $CuSO_4.5H_2O$
- 0.00004g $CoCl_2.6H_2O$

The pH of the minimal salt media is 7.

5.3 Culture medium using CO_2 as carbon source

Maintenance medium: The culture medium used for maintaining the algal culture was prepared by sparging pure CO_2 into M18 medium for 10 hours. In order to acclimatise the algal strain, the organism was maintained in this medium under constant illumination of 2.5kLux at 37℃. The culture medium for conducting the experiments by varying the CO_2 concentrations was prepared by sparging the M-18 medium for 10 hours with CO_2-Air mixture containing different partial pressures of CO_2. The CO_2 equilibrium concentration values in the aqueous phase have been determined using Henry's law (Sander, 2015).

5.4 Determination of liquid phase CO_2 concentration under equilibrium

Assuming that Henry's law is valid and the attainment of equilibrium, aqueous phase concentration of CO2 corresponding to different inlet concentration or partial pressure of CO_2 in the inlet air-CO_2 mixture has been determined as follows:

$$C^*_{L_{CO_2}} = H^{CP}_{CO_2} p_{CO_2} \quad (4)$$

Where,

$C^*_{L_{CO_2}}$ = Liquid phase concentration of CO_2 under equilibrium (moles)

p_{CO_2} = Partial pressure of CO_2 ingas phase (kPa)

$H_{CO_2}^{CP}$ = Henry's constant for CO_2 (moles/kPa)

Temperature dependence of

$$H_{CO_2} = H_{CO_2}^{\mathrm{Ref}} \exp\left[\frac{-\Delta \mathrm{H}_{Sol_{CO_2}^n}}{R}\left(\frac{1}{T} - \frac{1}{T^{\mathrm{Ref}}}\right)\right] \quad (5)$$

Where,

T^{Ref} = 298K

$\mathrm{H}_{CO_2}^{\mathrm{Ref}}$ = Henry's constant at 298K

From standard table (Sander, 2015):

$H_{CO_2}^{\mathrm{Ref}}$ = 3.3 x 10^{-4} M/KPa

$$\frac{-\Delta \mathrm{H}_{Sol_{CO_2}^n}}{R} = \frac{d \ln \mathrm{H}_{CO_2}}{d\left(\frac{1}{T}\right)} = 2400K$$

$H_{CO_2}^{310K}$ = 2.448 x 10^{-4} M/kPa (6)

The values of equilibrium concentration of CO_2 in aqueous phase corresponding to each gas phase concentration in CO_2-air mixture has been provided in Table 1 below.

Table 1: Values of equilibrium concentration of CO_2 in aqueous phase and volume of glycerol corresponding to each gas phase concentration in CO_2-air mixture

Gas phase in CO_2-Air concentration of CO_2 mixture% (v/v)	**5%**	**10%**	**15%**	**20%**	**100%**
Partial pressure of CO_2 (KPa)	5.065	10.13	15.195	20.26	101.3
Aqueous phase concentration of CO_2 (M)	0.00124	0.00248	0.00372	0.00495	0.02481
C_{gly}**, concentration of glycerol corresponding to gas phase concentration of CO_2-air mixture (M)**	0.413304 x 10^{-3}	0.82660 x 10^{-3}	1.23991 x 10^{-3}	1.65321 x 10^{-3}	8.2701 x 10^{-3}
V_{gly}**, volume of glycerol used per litre of photoheterotrophic medium (mL)**	0.030177	0.06038	0.09053	0.1207	0.60385

5.5 Experimental setup of photo autotrophic batches

250 ml conical flasks were used as algal bioreactors. The working volume was maintained at 150 ml for all the experiments. Each of the flasks was equipped with two glass tubes affixed

to a cork; one for transfer of inoculum and the other for transfer of CO_2. An outlet was also provided at the bottom of the conical flask as shown in Figure 6.

Figure 8: Photoautotrophic batch set up

At the beginning of each batch run, the conical flasks were rinsed and dried followed by filling them to the brim with the minimal salt media having saturated CO_2 as described in eqn. (4). 1g of algal inoculum was transferred into one of the glass tubes and the cork holding the tubes was placed on the beaker such that the inoculum tube is submerged below the 150 ml mark on the conical flask. The setup was checked for any leakages at the junction and identified leakages were sealed using parafilm and silicon grease. Air-CO_2 mixture consisting of varying gas phase CO_2 concentrations (5% to 20% (v/v)) were then introduced in the conical flasks using the gas transfer tube which displaces M-18 media to create a headspace containing the gas mixture. The outlet valve of the conical flask was opened to aid the displacement of the media as well as to normalize the pressure build-up inside the flask. The inlet pipe was then clamped using pinch-cocks so as to eliminate any chance of leakage due to back flow. The algal biomass was introduced in the conical flasks by the movement of the piston of an injection vial filled over the biomass with M-18 media so as to wash out the biomass present in the inoculum tube. Algal growth in culture medium having saturated liquid phase concentration of CO_2 against each gas phase concentration 5-20%) was conducted for different time periods up to 4 days. For each gas phase concentration (5-20%) of CO_2, four sets of experiments were conducted for 1,2,3, and 4 days. Constant illumination of 2.5kLux and temperature of 37°C were maintained during all growth experiments. Growth

medium for each time duration was analysed for algal mass and its lipid content.

5.6 Culture medium for photoheterotrophic growth

Growth medium for photoheterotrophic growth was prepared by supplementing M-18 medium with glycerol instead of CO_2 as carbon source. The values of concentrations of glycerol were maintained at levels to supply equal number of gram atoms of carbon which was available in the aqueous phase corresponding to different gas phase concentration (5-20%) of CO_2, as used in photoheterotrophic growth. Equivalent glycerol concentration against each gas phase concentration of CO_2 has been calculated using the following equation.

$$C_{gly} = \frac{p_{CO_2} \times H_{CO_2}^{CP} \times n_{C_{CO_2}}}{n_{C_{gly}}} \tag{7}$$

Where,

C_{gly} = glycerol concentration (moles)

$n_{C_{gly}}$ = number of gram atoms of carbon in one mole glycerol

$n_{C_{CO_2}}$ = number of gram atoms of carbon in one mole CO_2

p_{CO_2} = Partial pressure of CO_2 ingas phase (kPa)

$H_{CO_2}^{CP}$ =Henry's constant for CO_2 (moles/kPa)

The values of C_{gly} was maintained for substitution of C, available at different gas phase concentration (5-20%) of CO_2 used under the present study. Volume of glycerol (V_{gly}) required for 1L photoheterotrophic solution (glycerol supplemented M-18) was as follows,

$$V_{gly} = C_{gly} \times \frac{MW_{gly}}{\rho_{gly}} \tag{8}$$

Where,

C_{gly} = glycerol concentration (moles)

MW_{gly} = molecular weight of glycerol (g/moles)

ρ_{gly} = density of glycerol (g/mL)

5.7 Experimental setup of photo heterotrophic batches

60 ml culture tubes were filled with 30 ml volume of M-18 minimal salt media containing

glycerol. The values of V_{gly} used for substitution of C supplied by gas phase having different CO_2 concentrations have been provided in Table 1. 0.2 g of algal biomass was inoculated in each of the tubes as seen in Figure 7.

Figure 9: Photoheterotrophic batches inside the incubator

The headspace was sparged with argon to remove any trace of carbon dioxide or other gases present in the headspace. The tubes were closed using caps and sealed with parafilm. The tubes were then carefully placed as slants inside an incubator and incubated at 37°C for duration up to 4 days under illumination of 2.5kLux. For each concentration of glycerol 4 sets of experiments varying time duration of 1, 2, 3 and 4 days were conducted. Each growth medium was analysed for biomass concentration and the corresponding lipid content.

5.8 Orsat analysis

The orsat apparatus contains a water jacketed measuring bottle that is connected to a three-way manifold at top linking it to the three absorption pipettes. The setup also consists of a levelling bottle that is used for adjusting as well transferring sample gas volume into the measuring vessel as well as the absorption pipettes. The set consists of three-way stopcock that can be used introducing the gas sample as well as removing residual sample after estimation the constituents of the gas sample. In order to measure the CO_2 sequestration capability of *L. subtilis JUCHE1*, only CO_2 and O_2 will be analysed. The adsorbent used for CO_2 is caustic potash solution prepared by dissolving 250 gm KOH in 500 ml of distilled water. In case of estimating O_2, alkaline pyrogallol solution is used which is prepared by dissolving 25gms of pyrogallic acid in 500ml of KOH solution. The third absorbent pipette was filled with water as carbon monoxide is not to be analysed. The adsorbent levels in the pipettes are adjusted to coincide with marks below the stopcocks using the levelling bottle. The gas sample is collected by connecting the U-tube of the apparatus with the gas inlet tube

in the photoautotrophic setup. When the measuring burette reads 0, it can be confirmed that 100ml of sample has been transferred into the apparatus. In order to determine percentage of CO_2 left in the collected gas sample, the levelling bottle is raised slightly and the stopcock attached to KOH solution pipette is opened. The gas is passed forward and backwards many times by using the levelling bottle. The gas is brought back to the burette till the KOH solution reaches the mark on the capillary tube at which point the stopcock is closed. The contraction in volume in the burette caused when the gas is brought to the atmospheric pressure by levelling the liquid level in the levelling bottle with the liquid level in the measuring burette. The % CO_2 present in the gas sample can be estimated using the following equation:

$$\%CO_2 \text{ uptake efficiency} = \frac{Inlet_{CO_2} - Outlet_{CO_2}}{Inlet_{CO_2}} \times 100 \quad (9)$$

Where,

$Inlet_{CO_2}$ = Initial CO_2 concentration (%v/v)

$Outlet_{CO_2}$ = Final CO_2 concentration (%v/v)

5.9 Determination of Growth kinetic parameters

The difference between the final weight of Petri plate along with the sample after drying ($C_{X_{Final}}$) and the initial dry weight of the Petri plate ($C_{X_{Initial}}$) was noted at each interval to obtain the dry weight of the biomass.

Hence, biomass concentration:

$$C_X = C_{X_{Final}} - C_{X_{Initial}} \quad (10)$$

The biomass productivity can be calculated using the formula:

$$P_{Biomass} = \frac{\Delta C_X}{\Delta t} \quad (11)$$

Where,

$P_{Biomass}$ = Biomass productivity ($gL^{-1}day^{-1}$)

ΔC_X = Change in biomass concentration during time interval Δt (g/L)

The biomass concentration can be used for finding out the specific growth rate by using the formula (Kargi & Shuler, 1992):

$$\mu = \frac{1}{\overline{C_X}} . \frac{\Delta C_X}{\Delta t} \quad (12)$$

Where,

μ = Specific growth rate (day^{-1})

$\overline{C_X}$ = Average biomass concentration at a time interval (g/L)

ΔC_X = Change in biomass concentration during time interval Δt (g/L)

Monod's kinetic equation is normally used for determining the value of μ_{max} and K_s:

$$\mu = \frac{\mu_{\max} . S}{K_S + S} \tag{13}$$

Where,

$\mu_{\max}$ = Maximum specific growth rate (day^{-1})

S = Concentration of substrate (g/L)

K_S = Substrate saturation rate constant (g/L)

Reciprocal of the equation above yields:

$$\frac{1}{\mu} = \left(\frac{K_s}{\mu_{\max}} \right) . \frac{1}{S} + \frac{1}{\mu_{\max}} \tag{14}$$

This closely resembles

$$y = mx + c$$

This gives us,

$$\text{Slope (m)} = \frac{K_s}{\mu_{\max}} \tag{15}$$

$$\text{Intercept (c)} = \frac{1}{\mu_{\max}} \tag{16}$$

The solution the above equation helps in finding out the maximum specific growth rate (μ_{max}) and half saturation rate constant or Monod's constant (K_S). In case of substrate inhibition (Kargi & Shuler, 1992), Haldane's uncompetitive substrate inhibition equation is followed:

$$\mu = \frac{\mu_{\max} S}{S + K_S + \frac{S^2}{K_I}} \tag{17}$$

Where,

$\mu_{\max}$ = Maximum specific growth rate (day^{-1})

S = Concentration of substrate (g/L)

K_S = Half saturation rate constant (g/L)

K_I = Substrate inhibition constant (g/L)

The maximum substrate concentration at which substrate inhibition occurs can be determined using:

$$S_{max} = \sqrt{K_S . K_I} \quad (18)$$

Where,

S_{max} = Maximum substrate concentration (g/L)

5.10 Pigment extraction

Since the organism chosen for the experiment performs photosynthesis, it is safe to presume that the specimen should contain the photosynthetic pigments like Chlorophyll a, Chlorophyll b and carotenoids. In the present study, different solvents have been utilised to estimate the pigment content of the algal strain. 0.5g of dried biomass was weighed and homogenised with 10 ml of each extraction solvents (80% Acetone, 95% Ethanol, Diethyl-ether, Dimethyl-sulphide and Methanol).

Figure 10: Depigmentation of algal biomass using Acetone-NaOH mixture followed by filtering out of the depigmented biomass for lipid extraction

The homogenised mixture that was obtained was then centrifuged at 1000 rpm for 15 minutes. The supernatant that was obtained was separated and mixed with 4.5 ml of the respective solvent used for extraction. The pigment content was analysed using spectrophotometer (Perkin Elmer, USA). The following equations for the respective solvents can be used to determine the concentration of Chlorophyll a, Chlorophyll b and total carotenoids present in the sample (Sumanta *et al.* 2014):

- 80% acetone

$$Ch-a = 12.25A_{663.2} - 279A_{646.8}$$
$$Ch-b = 21.5A_{646.8} - 5.1A_{663.2} \quad (19)$$
$$C_{x+c} = (1000A_{470} - 1.82Ch-a - 85.02Ch-b)/198$$

- 95% ethanol

$$Ch-a = 13.36A_{664} - 5.19A_{649}$$
$$Ch-b = 27.43A_{649} - 8.12A_{664} \quad (20)$$
$$C_{x+c} = (1000A_{470} - 2.13Ch-a - 97.63Ch-b)/209$$

- Diethyl-ether (DEE)

$$Ch-a = 10.05A_{660.6} - 0.97A_{642.2}$$
$$Ch-b = 16.36A_{642.2} - 2.43A_{660.6} \quad (21)$$
$$C_{x+c} = (1000A_{470} - 1.43Ch-a - 38.87Ch-b)/205$$

- Dimethyl-sulphoxide (DMSO)

$$Ch-a = 12.47A_{665.1} - 3.62A_{649.1}$$
$$Ch-b = 25.06A_{649.1} - 6.5A_{665.1} \quad (22)$$
$$C_{x+c} = (1000A_{480} - 1.29Ch-a - 53.78Ch-b)/220$$

- Methanol

$$Ch-a = 16.72A_{665.2} - 9.16A_{652.4}$$
$$Ch-b = 34.09A_{652.4} - 15.28A_{665.2} \quad (23)$$
$$C_{x+c} = (1000A_{470} - 1.63Ch-a - 104.96Ch-b)/221$$

Where,

$Ch-a$ = Concentration of Chlorophyll a (µg/ml)

$Ch-b$ = Concentration of Chlorophyll b (µg/ml)

C_{x+c} = Concentration of total carotenoids (µg/ml)

A = Absorbance

5.11 Lipid extraction

After stripping off the pigments, the biomass was subjected to lipid extraction. For depigmentation process the dry biomass was treated with a 20ml mixture of 1% NaOH and Acetone in a 3:4 ratio (%v/v) and placed inside the hot air oven at 60^{o} C for around 1 hour [ref.]. A solution of chloroform and methanol in the ratio of 2:1(%v/v) was prepared and the algal biomass was added in the Chloroform-Methanol solution and homogenized for about 10 minutes which helps in disrupting the cell wall of algae which in turn allows for greater efficiency for extracting lipids.

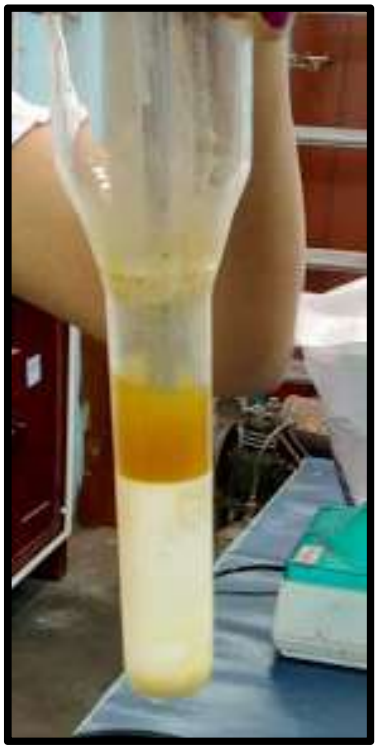

Figure 11: Homogenisation of depigmented biomass using Chloroform-Methanol mixture

After homogenization, the heterogeneous mixture was centrifuged for 15 minutes at 10,000 RPM in order to separate into supernatant which contains the lipids and the pellet containing the cell debris or cell hydrolysates.

Figure 12: Homogenised mixture being prepped for centrifugation

The supernatant was collected in a pre-weighed clean and dry beaker which was then transferred inside the hot air oven set at 60°C for removing the solvent present in extracted lipid and solvent mixture. The beaker is weighed again after the solvent completely evaporates.

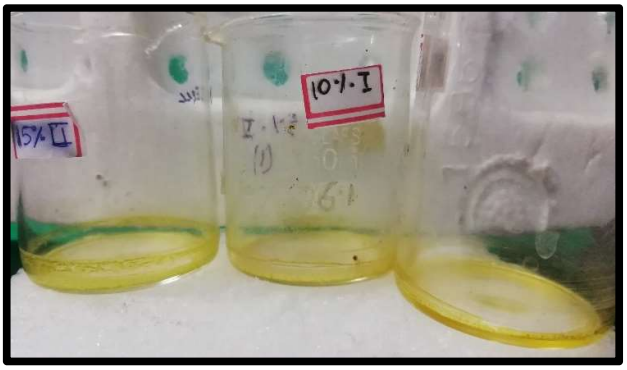

Figure 13: Supernatant containing algal lipid and extraction solvent post drying

The weight of extracted lipid can be calculated using:

$$\Delta L = L_f - L_i \quad (24)$$

Where,

ΔL = Weight of extracted lipid

L_f = Dry weight of beaker + extracted lipids (g)

L_i = Dry weight of the beaker (g)

The lipid content was calculated by the following equation given below:

$$\text{Lipid content (\%w/w)} = \frac{\Delta L}{C_X} \times 100 \quad (25)$$

Where,

ΔL = Weight of extracted lipid (g)

C_X = Dry cell weight at time t (g)

The lipid productivity can be easily calculated by the following equation:

$$P_{Lipid} = P_{Biomass} \text{ . Lipid content} \quad (26)$$

Where,

P_{Lipid} = Lipid productivity ($gL^{-1}day^{-1}$)

$P_{Biomass}$ = Biomass productivity in ($gL^{-1}day^{-1}$)

5.12 Determination of lipid kinetic parameters

The dried lipid weight was noted daily by subtracting the initial dry weight of the beaker from the dry weight of the centrifuged supernatant poured in the beaker after the extraction process. This allows determining the lipid content from the batches over the incubation period. Hence, this information can be used to calculate the specific rate of lipid formation

(q_p).

$$q_p = \frac{1}{\overline{C_X}} \cdot \frac{\Delta L}{\Delta t} \tag{27}$$

Where,

q_p = Specific rate of lipid formation (day^{-1})

ΔL = Change in lipid concentration in the time interval Δt (g/L)

$\overline{C_X}$ = Average biomass concentration at a time interval (g/L)

In case of substrate inhibition, Haldane's uncompetitive substrate inhibition equation is followed:

$$q_p = \frac{q_{p_{\max}} S}{S + K_s + \frac{S^2}{K_i}} \tag{28}$$

Where,

$q_{p_{\max}}$ = Maximum specific rate of lipid formation

S = Concentration of substrate

K_s = Half saturation rate constant

K_i = Substrate inhibition constant

The maximum substrate concentration above which substrate inhibition occurs can be determined using:

$$S_{\max} = \sqrt{K_s . K_i} \tag{29}$$

Where,

$S_{\max}$ = Maximum substrate concentration

Chapter 6: Results and discussions

6.1 Photo autotrophy in *L. subtilis JUCHE1*

The dry biomass weight of the CO_2 assisted batches have been evaluated using eqn. (10) and noted down in a tabulated format as seen in Table 2.

Table 2: Biomass concentration in different CO2-Air mixtures obtained upto 4 days of incubation

Days	Biomass concentration (g/L)			
	5% CO_2	**10% CO_2**	**15% CO_2**	**20% CO_2**
0	0.2473	0.2473	0.2473	0.2473
1	0.394	0.434	0.4333	0.538
2	0.4833	0.674	0.7246	0.6366
3	0.5653	0.5906	0.5186	0.5634
4	0.6068	0.68595	0.496	0.5013

The initial dry biomass concentration was noted to be 0.2473 g/L for all the batches. From the biomass concentration vs time graph, it was clearly observed that the biomass concentration for all the batches having different inlet CO_2 concentrations initially increases with increase in substrate concentration (5-20%) CO_2-air ratios. In case of 10%, 15% and 20% batches, as evident from Figure 14, the biomass concentration peaked on day 2 after which there is an observable decline in concentration. On basis of Figure 14, it should be noted that after 4 days of incubation, only 5% batch showed an increasing trend signifying that the biomass may still be in exponential phase while in case of 15% and 20%, the biomass might have entered stationery and subsequently death phase after 2nd day. In case of 5% and 10% CO_2 batches the highest biomass concentrations were obtained on 4th day i.e. 0.6068 g/L and 0.68595 g/L respectively. In 15% and 20% batches, the highest biomass concentration obtained on 2nd day for both batches were 0.7246 g/L and 0.6366 g/L respectively. Among the experimental runs conducted by varying the inlet CO2 concentrations in the range of 5-20%, the highest biomass concentration was observed to be 0.7246 g/L for 15% CO_2 inlet concentration. Therefore, it can be inferred that 15% inlet CO_2-Air mixture is the optimum substrate concentration for biomass growth.

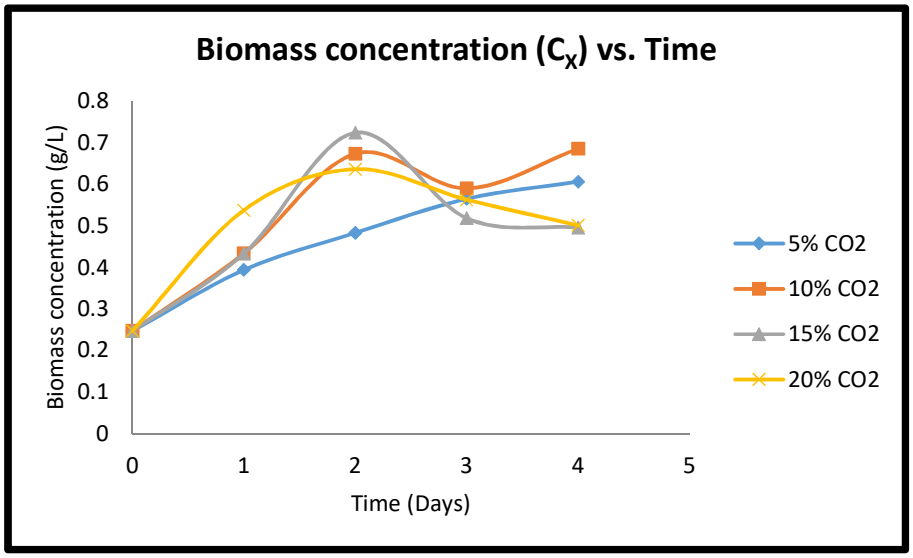

Figure 14: Biomass concentration of *L. subtilis JUCHE1* in different gas phase CO_2-air mixture vs. Time

The biomass concentration data is utilised for determining the biomass productivity which denotes the rate of biomass generation within an ecosystem. By evaluating biomass productivity ($P_{Biomass}$) using eqn. (11), and plotting it against time helps in investigating the ability of *L. subtilis JUCHE1* to undergo cell division in different CO_2-Air ratio concentration can be determined. As evident in the Figure 15, the maximum biomass productivity for 5% and 20% batches can be observed on 1st day while in case of 10% and 15% CO_2 batches, the biomass productivity peaks on 2nd day. The highest biomass productivity that has been observed in the photoautotrophic batches is 0.2913 g/L/day for 15% batch on 2nd day. Since there is a decline in biomass concentration as seen in Figure 14, it can be noted that with decrease in biomass concentration with respect to time, the rate of biomass productively also declines.

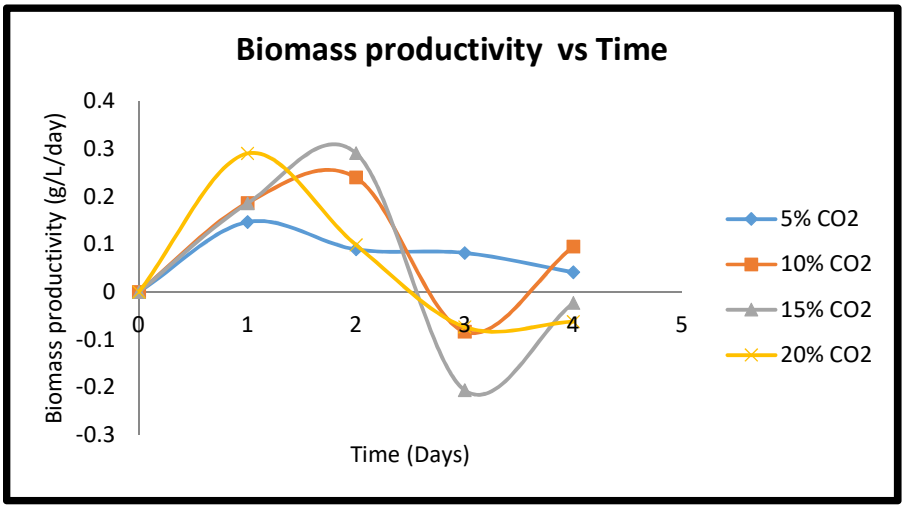

Figure 15: Biomass productivity *L. subtilis JUCHE1* in different gas phase CO_2-air mixture vs. Time

The biomass concentration has been used to determine the specific growth rates (μ) using eqn. (12). Figure 16 depicts the plot of μ vs. S, which shows that with increase in substrate concentration, the organism shows substrate inhibition which is evident from the bell-shaped curve. The maximum substrate concentration till which the organism shows growth is 15% CO_2-Air ratio after which the growth rate declines.

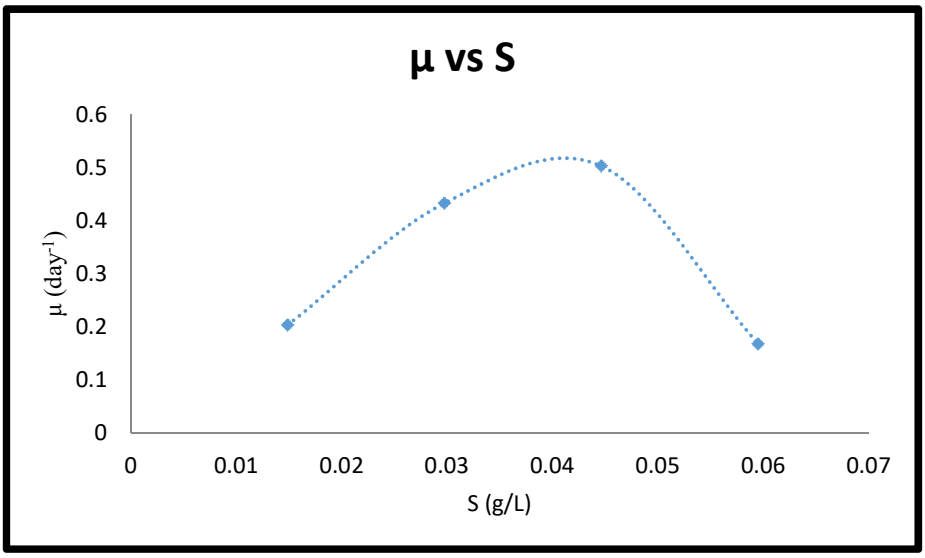

Figure 16: Specific growth rate (μ) of *L. subtilis JUCHE1* vs. concentration of carbon present in liquid phase CO_2 (S)

By plotting 1/μ vs. 1/S as shown in Figure 17, it is possible to determine the value of maximum specific growth rate (μ_{max}) and saturation rate constant (K_S). The value of μ_{max} has been found out to be 3.667 day^{-1} and K_S has been evaluated to be 0.24972 g/L. Since the maximum substrate concentration is known, eqn. (18) can be used to determine the inhibition constant (K_I) in non-competitive substrate inhibition. The inhibition constant has been

evaluated to be 0.007965 g/L.

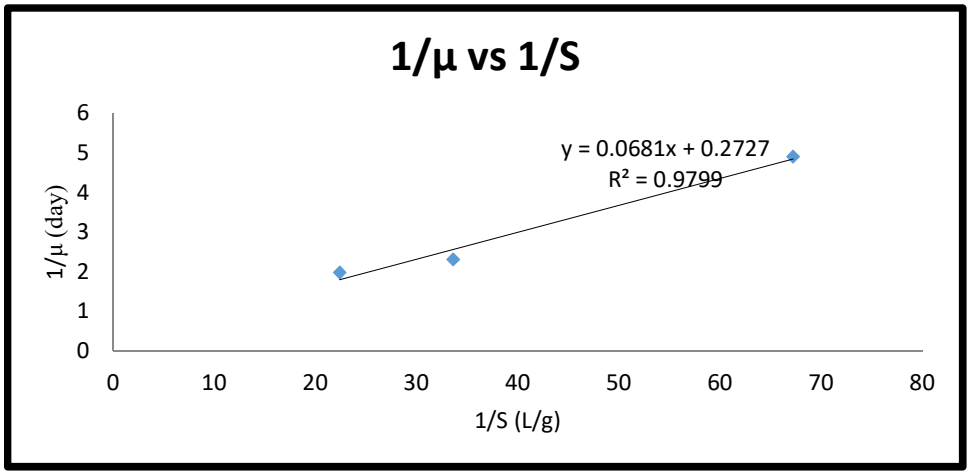

Figure 17: Double reciprocal plot of specific growth rate (μ) and concentration of carbon present in liquid phase CO_2 (S)

The weight of lipid extracted at the end of each batch study has been calculated using eqn. (24). From Table 3, it can be inferred that the initial lipid concentration is 0.01 g/L for all the batches. The dry weight of extracted lipid can be used for determining the lipid content using eqn. (25).

Table 3: Lipid concentration of *L. subtilis JUCHE1* in different gas phase CO_2-air mixture over the incubation period

Days	Lipid concentration (g/L)			
	5% CO_2	10% CO_2	15% CO_2	20% CO_2
0	0.01	0.01	0.01	0.01
1	0.021333	0.029933	0.034333	0.024
2	0.017533	0.0288	0.054393	0.022
3	0.003	0.015867	0.040133	0.016667
4	0.002333	0.0156	0.061993	0.005333

It was observed that the maximum lipid was extracted in 15% CO_2 batch i.e. 0.061993 g/L on 4^{th} day. By plotting lipid content vs. time, it was observed that the highest lipid content was 12.499% (w/v) for 15% CO_2 batch on 4^{th} day. In case of the rest of the batches (5%, 10% and 20%), it can be deduced from the Figure 18, the lipid contents peaked on 1^{st} day after which the content declines with respect to time.

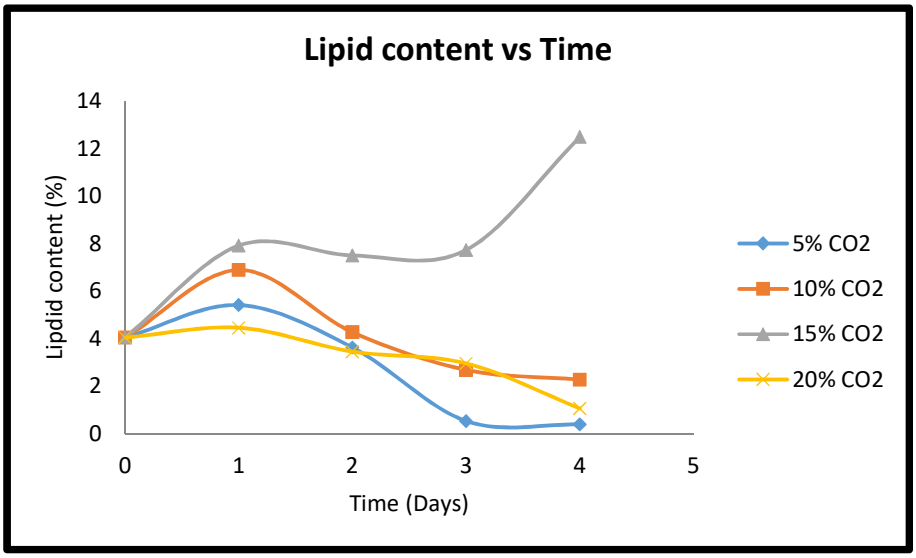

Figure 18: Lipid content of *L. subtilis JUCHE1* in different gas phase CO_2-air mixture vs. Time

The lipid content can be utilised to determine the lipid productivity by using eqn. (26). It was observed that the lipid productivity for 5%, 10% and 20% batches were highest on 1st day after which the productivity declines with time as evident in Figure 19. However, in case of 15% CO_2 batch, the maximum productivity of 0.0219 g/L/day was observed on the 2nd day. Since lipid productivity is a function of biomass productivity, the trends in lipid productivity follows trend similar to that of biomass productivity.

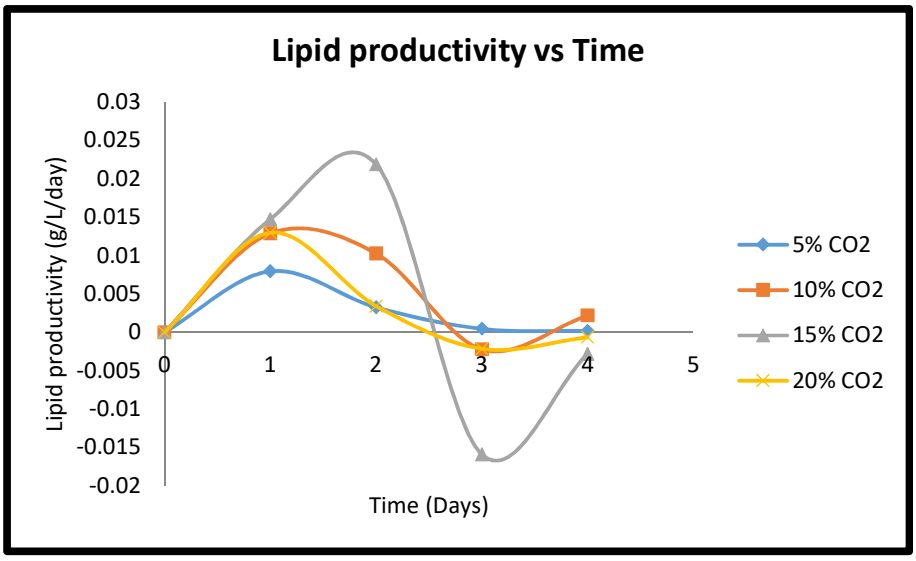

Figure 19: Lipid productivity of *L. subtilis JUCHE1* in different gas phase CO_2-air mixture vs. Time

Since biomass concentration and lipid concentration data are available, it is possible to calculate the specific rate of lipid formation (q_p) using the eqn. (27). By plotting q_p vs. substrate concentration (S) as seen in Figure 20, it can be clearly observed that the curve is

bell shaped which suggests that there has been substrate inhibition.

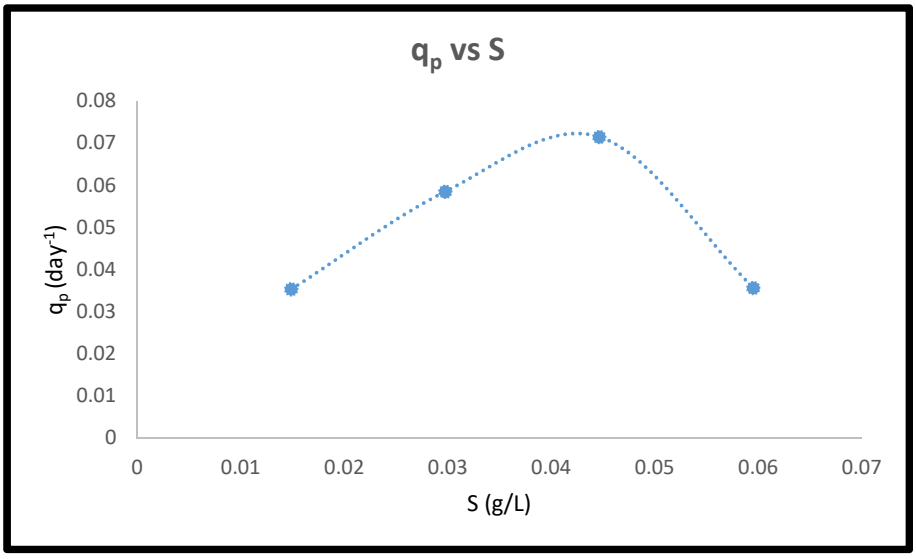

Figure 20: Specific rate of lipid formation (q_p) vs concentration of carbon present in liquid phase CO_2 (S)

It can be clearly noted that the q_p vs. S curve peaks at 15% CO_2 concentration and the peak q_p has been determined to be 0.071506 day^{-1}. Similar to determining the maximum specific growth rate, the maximum specific rate of lipid formation can be determined by plotting $1/q_p$ vs. 1/S as shown in Figure 14.

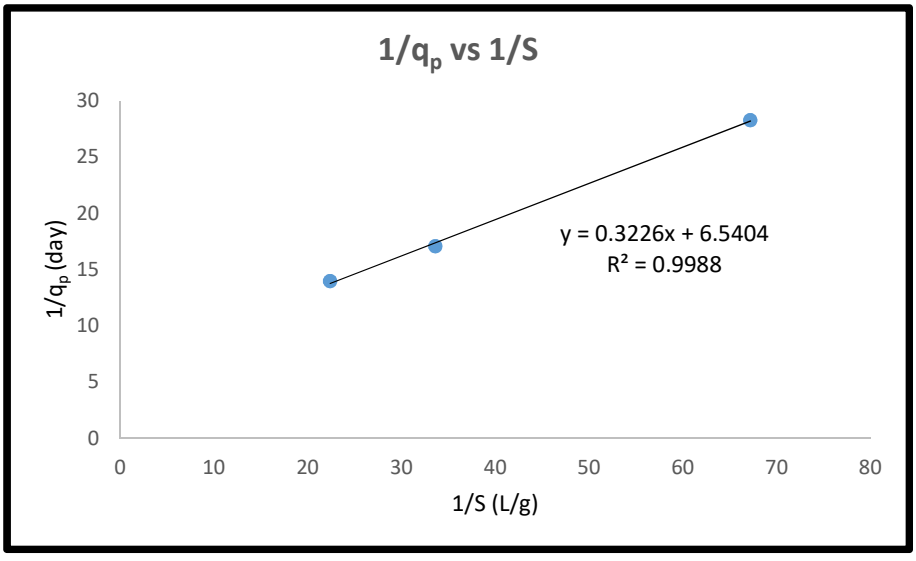

Figure 21: Double reciprocal plot of lipid formation (q_p) vs concentration of carbon present in liquid phase CO_2 (S)

By plotting $1/q_p$ vs. 1/S, it is possible to assess the trend line equation of the plot. By solving the established equation, the value of $q_{p\ max}$ has been found out to be 0.15289 Day^{-1}. Similarly, the half saturation constant (K_s) has been determined to be 0.04932 g/L. Since, the value of maximum substrate concentration (S_{max}) beyond which inhibition occurs and K_s is

known, the value of K_i for lipid kinetics can be easily determined using eqn. (29). K_i has been determined to be 0.0404 g/L.

6.2 CO_2 uptake ability and efficiency in *L. subtilis JUCHE1*

In photoautotrophic batches, one of the primary investigations carried out was determining the CO_2 uptake and sequestration ability of the algal strain.

Table 4: CO_2 uptake efficiencies in different CO_2-Air mixture

Days	5% CO_2	10% CO_2	15% CO_2	20% CO_2
0	0	0	0	0
1	32	42	50	53
2	56	48	66.66667	60
3	68	64	76.66667	65.5
4	84	72	96	88

As seen in Table 4, it can be seen that *L. subtilis JUCHE1* shows a good uptake efficiency. The maximum efficiency of 96% was observed for 15% CO_2 batch.

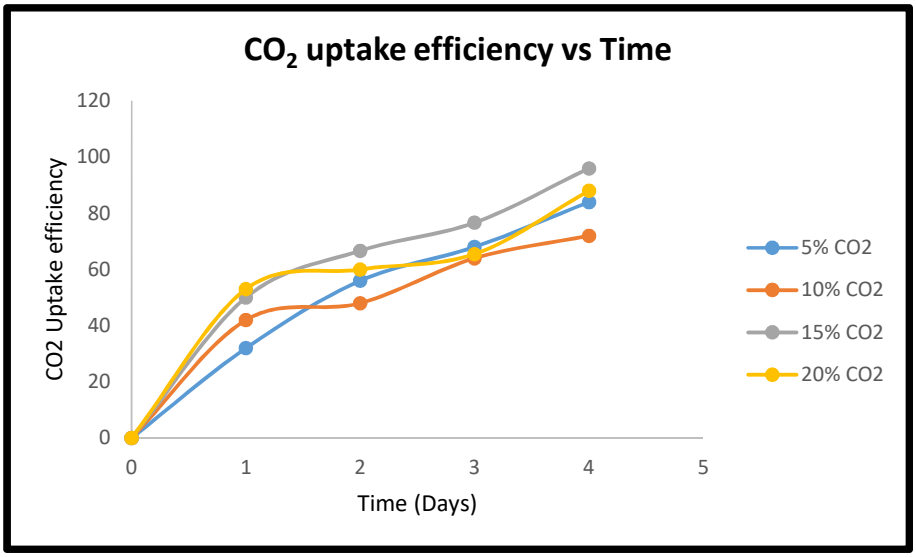

Figure 22: CO_2 uptake efficiency vs. Time

6.3 Photo heterotrophy in *L. subtilis JUCHE1*

Table 5: Biomass concentration of *L. subtilis JUCHE1* in equivalent glycerol concentration against each gas phase concentration of CO_2 vs Time

Days	Biomass concentration (g/L)			
	5% Glycerol	10% Glycerol	15% Glycerol	20% Glycerol
0	0.2473	0.2473	0.2473	0.2473
1	0.422	0.493023	0.520667	0.447333
2	0.588	0.768822	0.665333	0.561067
3	0.652633	0.772767	0.6824	0.6595
4	0.746	0.785733	0.817	0.741333

In the photoheterotrophic condition, the culture medium is supplemented by glycerol containing equivalent gram atoms of carbon present in different gas phase concentration of CO_2 (5-20%) in aqueous phase. When the microalgae were grown in glycerol assisted medium, the biomass concentration data for each of the different substrate concentrations were noted down for each of the batches. The initial biomass concentration was calculated to be 0.2473 g/L for each of the substrate concentrations. It can be clearly observed in Figure 23 as well as Table 5, the biomass concentration in each substrate concentration increases from day zero to day four. The maximum biomass concentration for 5%, 10%, 15% and 20% glycerol batches were obtained on 4^{th} day in each batch i.e. 0.746 g/L, 0.785733 g/L, 0.817 g/L and 0.741333 g/L respectively. The highest biomass concentration for the present experimental study was observed to be 0.817 g/L for 15% glycerol, which signifies that 15% glycerol is the optimum substrate concentration.

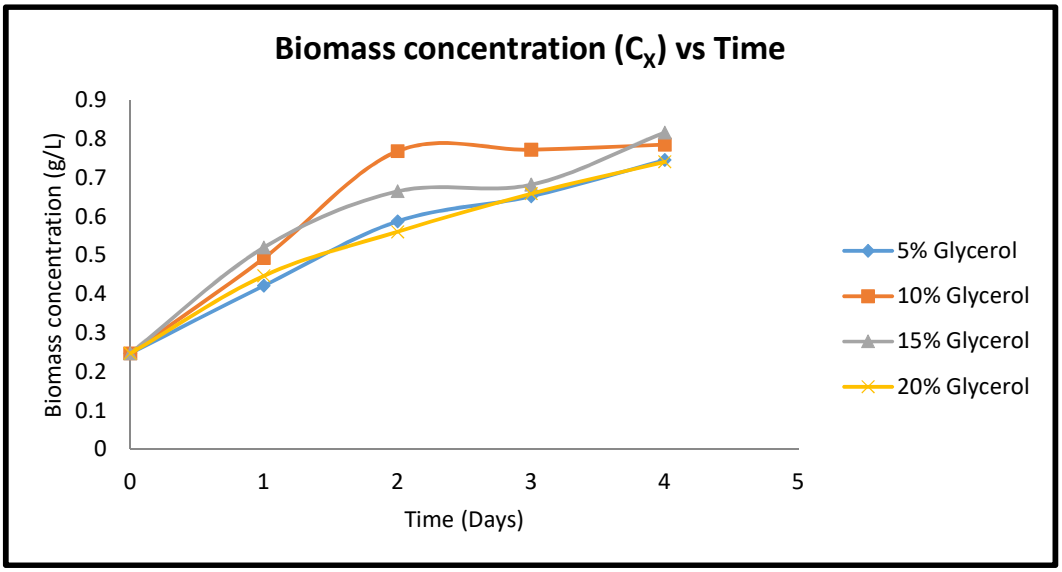

Figure 23: Biomass concentration of *L. subtilis JUCHE1* in equivalent glycerol concentration against each gas phase concentration of CO_2 vs Time

From Figure 23, it can be observed that the in glycerol assisted growth, the biomass concentration increases with time. However, in case of batch with 20% glycerol batch, the biomass concentrations are almost close to the biomass concentrations reported for 5% glycerol batch while at the same time they are significantly lower than biomass concentrations in 10% and 15% batches. It can also be observed that in 10% glycerol batch, after 2nd day, the biomass concentration remains largely unchanged which implies, that the organism begins entering the stationary phase. The same cannot be said for the other batches as the biomass concentration exhibits an increasing trend with respect to time. The biomass concentration is a vital parameter to be considered when calculating growth kinetics of an organism. The growth rate (μ) values have been calculated for each of the batches by using eqn. (13). The substrate concentration (S) and μ are plotted against each other to infer whether the organism shows any inhibition to substrate concentration.

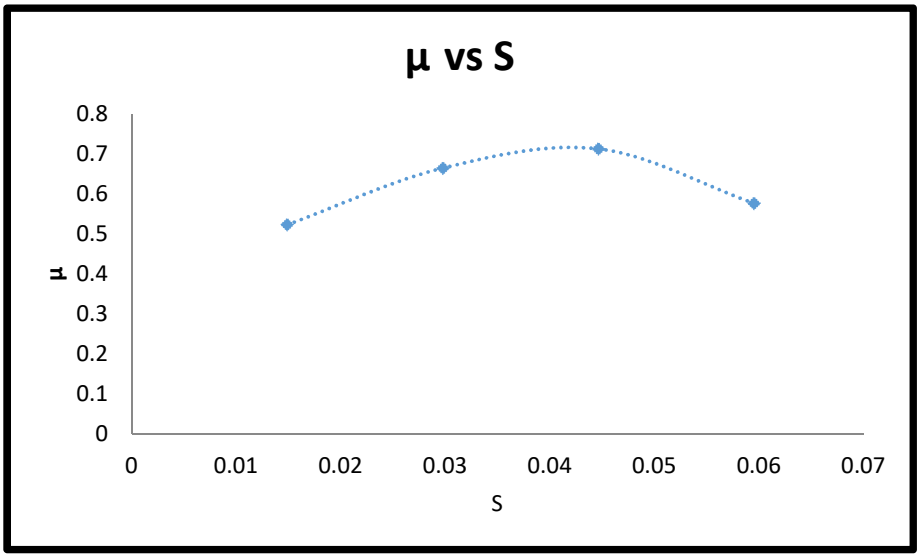

Figure 24: Specific growth rate (μ) of *L. subtilis JUCHE1* vs. concentration of carbon present in equivalent glycerol concentrations against each gas phase concentration of CO_2 (S)

Values of μ were obtained and plotting these values against substrate concentration yielded a bell-shaped curve. It can be clearly seen in Figure 24, that the peak of the curve was obtained at 15% glycerol concentration after which the curve declines. This shows that above 15% substrate concentration, the organism is inhibited. This figure also corroborates with Figure 23, where the biomass concentration in 20% batch was very less in comparison to the biomass concentrations obtained for the other batches. The maximum substrate concentration has been found out to be 15% glycerol concentration.

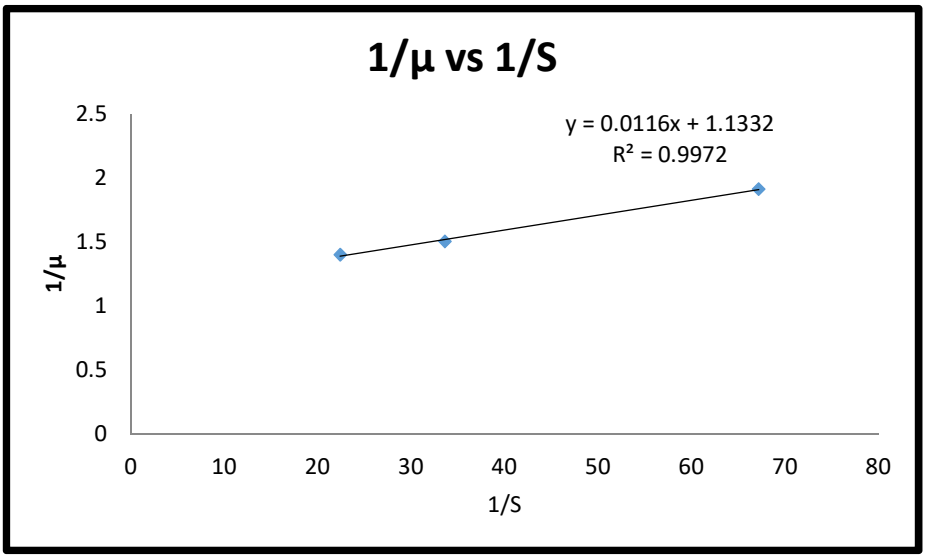

Figure 25: Double reciprocal plot of specific growth rate (μ) and concentration of carbon present in equivalent glycerol concentrations against each gas phase concentration of CO_2 (S)

After the μ vs. S plot, in order to determine the Monod constant (K_S) and maximum specific growth rate (μ_{max}), the reciprocal plot of 1/μ vs. 1/S was graphically represented in Figure 25. By using the trend line, the overall equation for the plot can be obtained. The equation can be solved for determining the value of μ_{max} which has been found out to be 0.8826125 day^{-1}. Similarly, the value of K_S has been found to be 0.01023 g/L. Since the values of K_S and maximum substrate concentration are known to us it enables us to determine the inhibition constant (K_i) using the eqn. (15). Solving the equation gives K_I to be 0.1945 g/L.

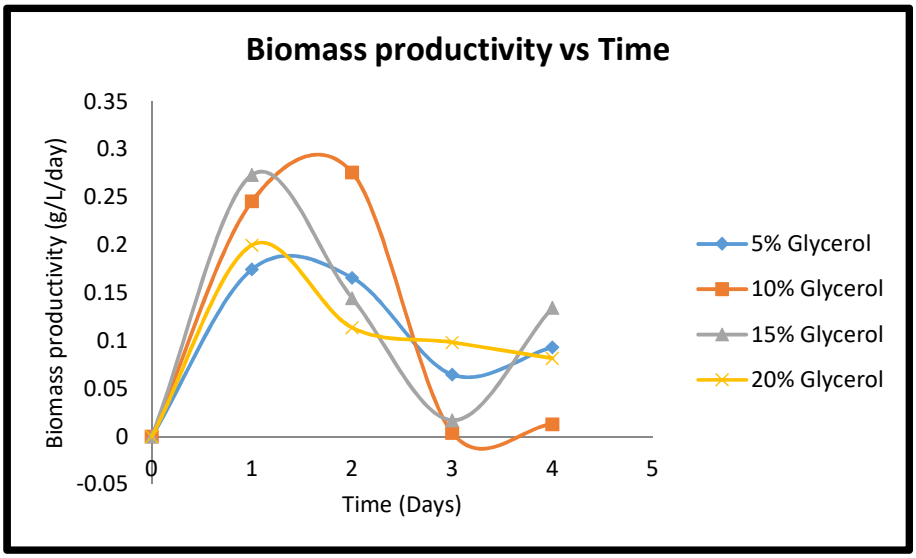

Figure 26: Biomass productivity of *L. subtilis JUCHE1* in equivalent glycerol concentration against each gas phase concentration of CO_2 vs Time

The biomass productivity ($P_{Biomass}$) has been calculated by putting the biomass concentration data in eqn. (11). From Figure 26, it can be noted that the highest biomass productivity for 5%, 15% and 20% substrate concentration has been observed on day 1 after which the productivity starts to decline with respect to time. The highest biomass productivity for 10% glycerol concentration has been observed on 2nd day after which the productivity declines similar to the other batches. The highest biomass productivity in the present study has been found out to be 0.275799 g/L/day for 10% glycerol batch.

Table 6: Lipid concentration of *L. subtilis JUCHE1* in equivalent glycerol concentration against each gas phase concentration of CO_2 vs Time

Days	Lipid concentration (g/L)			
	5% Glycerol	10% Glycerol	15% Glycerol	20% Glycerol
0	0.0096	0.0096	0.0096	0.0096
1	0.054	0.063333	0.061	0.054033

2	0.136333	0.13	0.108667	0.11
3	0.284733	0.170667	0.26	0.157
4	0.420333	0.220333	0.376667	0.213333

The weight of extracted lipid was calculated for each of the batch. The lipid data is useful in determining the lipid content in the biomass using eqn. (25). As it can be observed in Figure 27, the lipid content can be seen to increase with change in incubation time. The highest lipid content among all the batches was observed for 5% glycerol batch at 56.345% on 4th day. The maximum lipid content observed in 10%, 15% and 20% batches were 28.042%, 46.104% and 28.777% respectively on 4th day. Lipid content is used to determine the lipid productivity using eqn. (26).

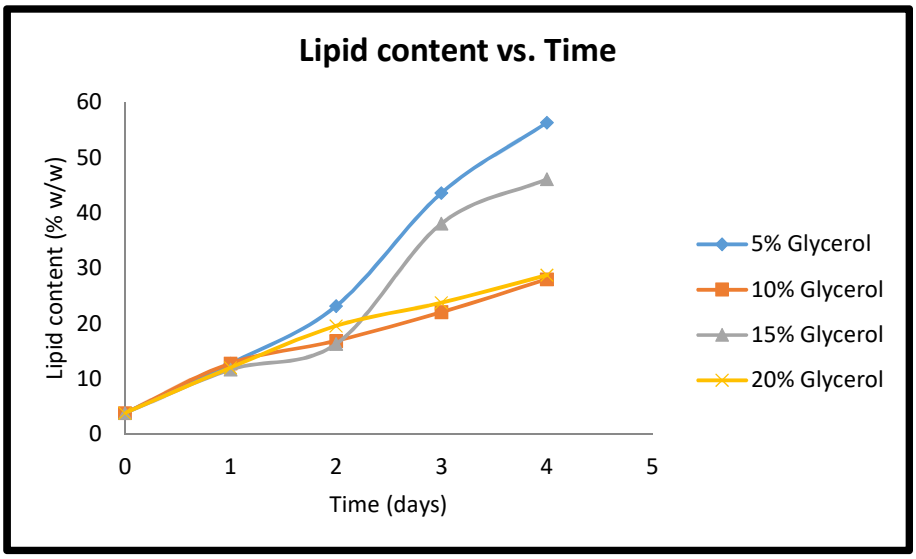

Figure 27: Lipid content of *L. subtilis JUCHE1* in equivalent glycerol concentration against each gas phase concentration of CO_2 vs Time

By observing Figure 28, it is clear that lipid productivity increases from day zero to day one for all the batches. However, the productivity declines in case of 15% and 20% batches right after day one. However, in case of 5% and 10% batch, the lipid content declines after 2nd day of incubation. As noted in equation (26), lipid productivity is directly proportional to the biomass productivity. This means irrespective of the lipid content; the lipid productivity trend will be very similar to the biomass productivity trends. The lipid productivity in 20% batch saturates after 2nd day, similar to the biomass productivity which also plateaus after 2nd day. However, on the basis of the lipid content, it can be inferred that the organism *L. subtilis JUCHE1* shows oleaginous traits when grown in glycerol assisted cultures.

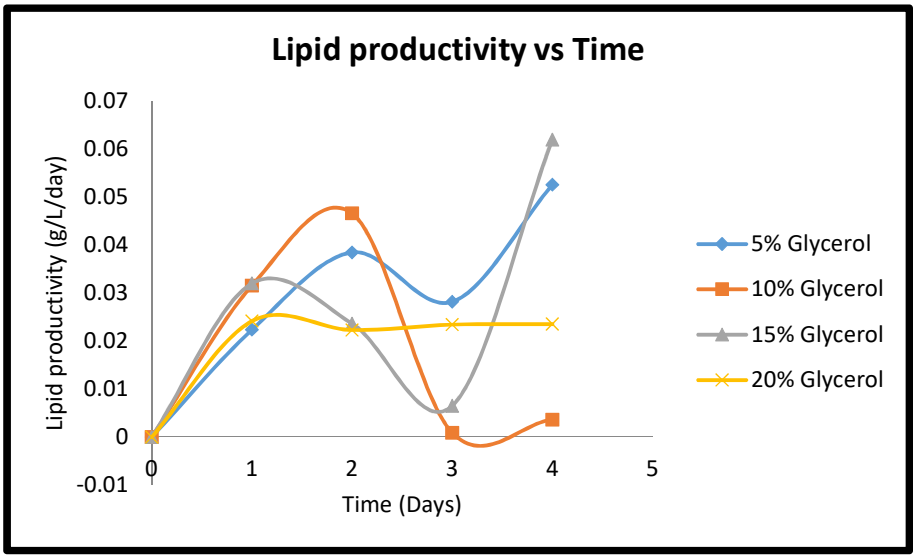

Figure 28: Lipid productivity of *L. subtilis JUCHE1* in equivalent glycerol concentration against each gas phase concentration of CO_2 vs Time

The lipid formation kinetics can be determined by evaluating q_p using eqn. (18) and plotting it against substrate concentration (S). As clearly seen in Figure 22, the curve is bell shaped which means that the organism encounters substrate inhibition beyond 15% glycerol concentration.

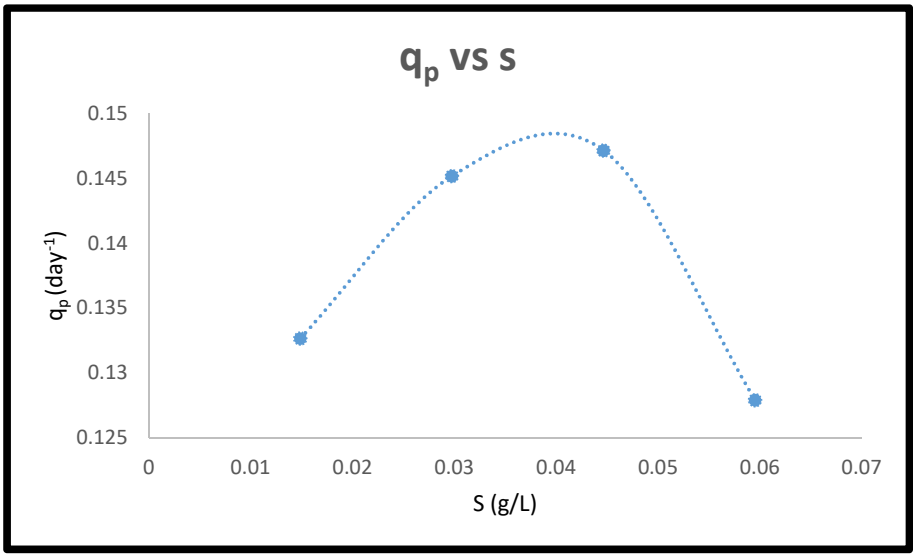

Figure 29: Specific rate of lipid formation (q_p) of *L. subtilis JUCHE1* vs. concentration of carbon present in equivalent glycerol concentrations against each gas phase concentration of CO_2 (S)

It is again possible to determine the values of maximum specific rate of lipid formation ($q_{p\,max}$) and substrate saturation rate constant by reciprocal plot of $1/q_p$ vs. 1/S.

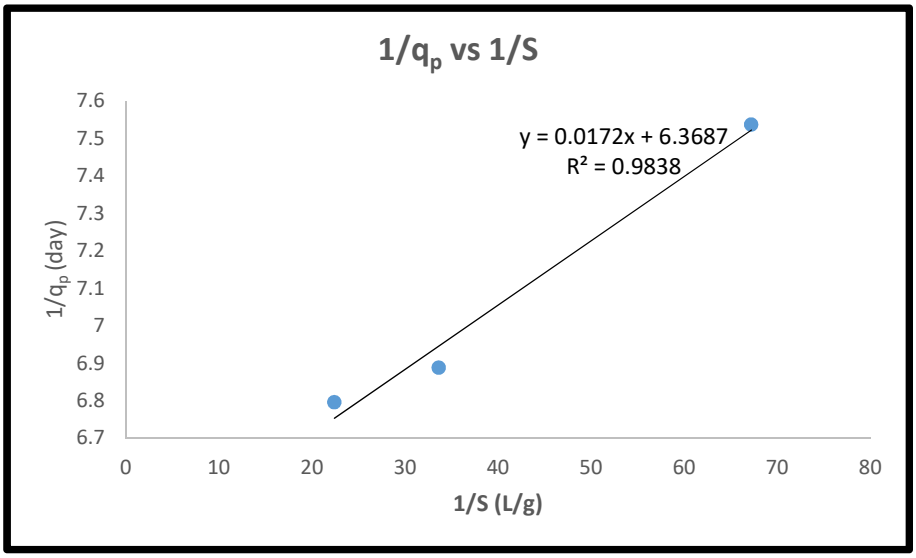

Figure 30: Double reciprocal plot of specific rate of lipid formation (q_p) of *L. subtilis JUCHE1* and concentration of carbon present in equivalent glycerol concentrations against each gas phase concentration of CO_2 (S)

By plotting $1/q_p$ vs. 1/S, it is possible to get a straight-line equation where the slope represents $\frac{K_s}{q_{p_{max}}}$ and the intercept represents $\frac{1}{q_{p_{max}}}$. Solving the equation gives the value of $q_{p_{max}}$ and K_s as 0.15701 day^{-1} and 2.7 x 10^{-3} g/L respectively. Since, it can be seen in Figure 22, that there has been substrate inhibition, it is possible to calculate K_i using the eqn. (29), since the value of the maximum substrate concentration above which inhibition occurs and half saturation rate constant is known. The K_i value has been evaluated to be 0.73804 g/L.

6.4 Extraction and quantification of pigments present in *L. subtilis JUCHE1*

The absorbance that was obtained for the extracted pigments has been substituted in eqn. (19), (20), (21), (22) and (23) to yield the concentration of Chlorophyll a (Chl-a), Chlorophyll b (Chl-b) and total carotenoids (C_{X+C}) in each of the respective extraction solvents.

Table 7: Concentration of Chlorophyll a (Chl-a), Chlorophyll b (Chl-b) and total carotenoids (C_{X+C}) extracted from *L. subtilis JUCHE1* using different extraction solvents

Solvents	Chl a (µg/ml)	Chl b (µg/ml)	C_{x+c} (µg/ml)
80% Acetone	5.06342218	1.920664	0.284473325
95% Ethanol	6.90805564	2.44542852	0.793594522
Methanol	2.24213736	1.98986136	0.045902569
Dimethyl sulphoxide	19.575803	8.201305	0.63893196

Diethyl ether	9.775123997	1.223601901	1.069112368

As it can be seen in Table 7, the maximum concentration of 19.575 µg/ml and 8.2013 µg/ml for Chl-a and Chl-b respectively were obtained in Dimethyl-sulphoxide (DMSO) suggesting that DMSO is a potential solvent for extracting Chl-a and b. The highest total carotenoids concentration was 1.0691 µg/ml in Diethyl ether. The Figure 31, graphically represents the findings of Table 7 for ease of understanding the comparison of the extraction ability of the different solvents used.

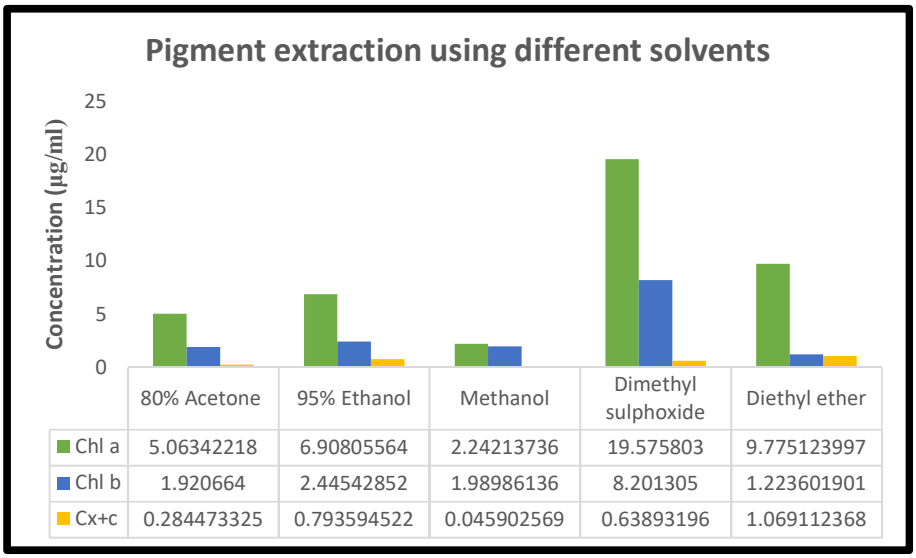

Figure 31: Graphical representation of concentration of pigments (µg/ml) extracted with respect top different extraction solvents

6.5 Algal lipid analysis using GC-MS analysis

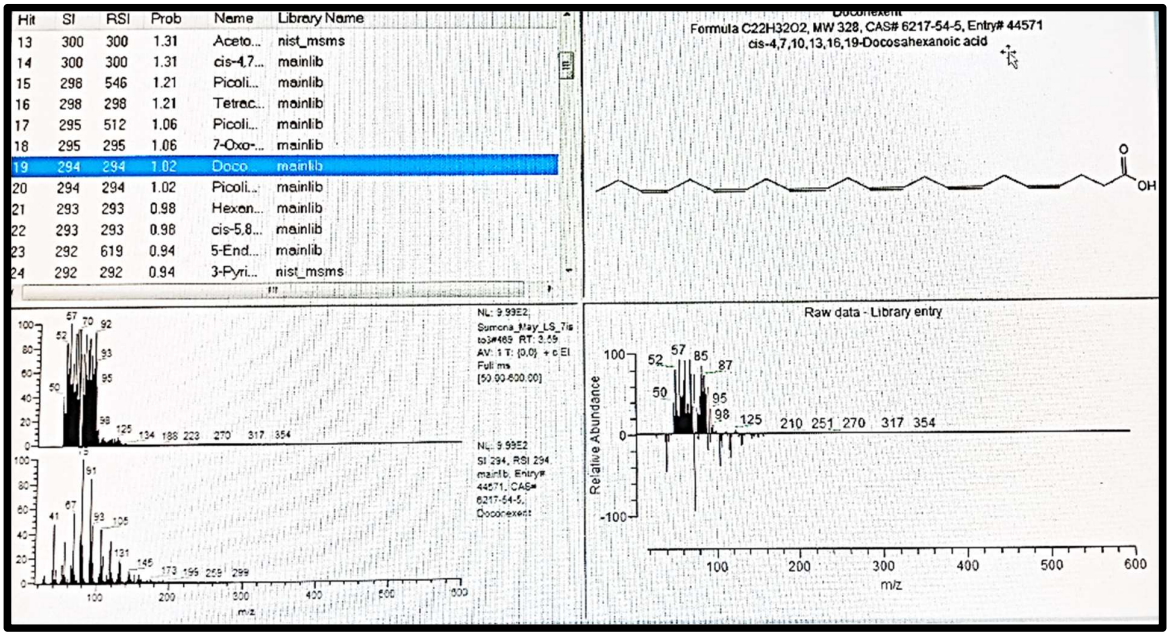

Figure 32: GC-MS analysis of algal oil

The algal lipid was characterised by using GC-MS analysis. According to Figure 32, it was found that the algal oil/lipid is rich in omega-3 fatty acid like DHA. The peaks obtained in the gas chromatography were compared with the mass spectrometry library for identifying Docosahexaenoic Acid (DHA) having retention time 3.59 min.

6.6 Curve fitting of experimental data on theoretical data

Table 8: Theoretical and experimental values of liquid phase CO_2 concentration (C_S), biomass concentration (C_X) and lipid concentration (C_L)

Day	Theoretical C_S	Theoretical C_X	Theoretical C_L	Experimental C_S	Experimental C_X	Experimental C_L
0	0.1637	0.2473	0.01	0.1637	0.2473	0.01
1	0.0807	0.3786	0.0288	0.081875	0.4333	0.034333
2	0.0292	0.4601	0.0429	0.027292	0.7246	0.054393
3	0.0089	0.4922	0.0491	0.016375	0.5186	0.040133
4	0.0025	0.5023	0.0512	0.031658	0.496	0.061993

It is evident from the tabulated data in Table 8 as well as the graphical representation of the same in Figure 33, Figure 34 and Figure 35, that the results of the experimental study actually follows a trend that is similar to the simulation results that has been obtained by solving the mass balance equations of liquid CO_2 concentration, biomass concentration and lipid

concentration using the ODE45 on MATLAB. On the basis of the figures presented it is justified to confer that the experimental results closely fit the theoretical results.

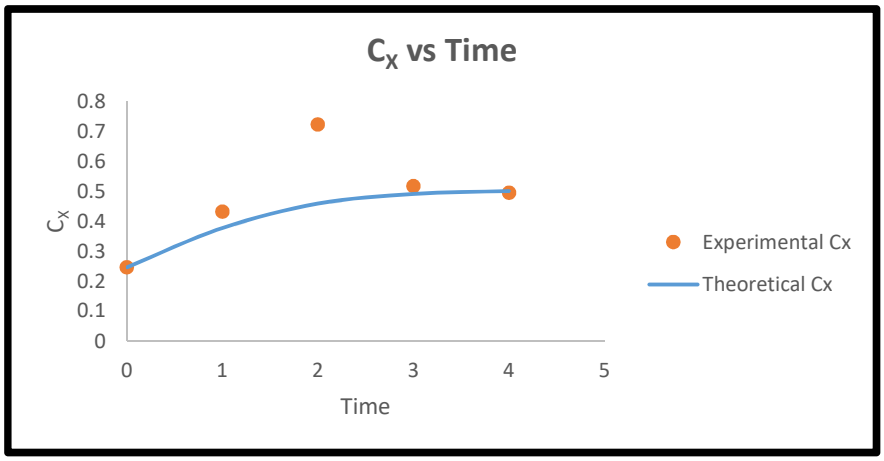

Figure 33: Theoretical and experimental biomass concentrations plotted against time

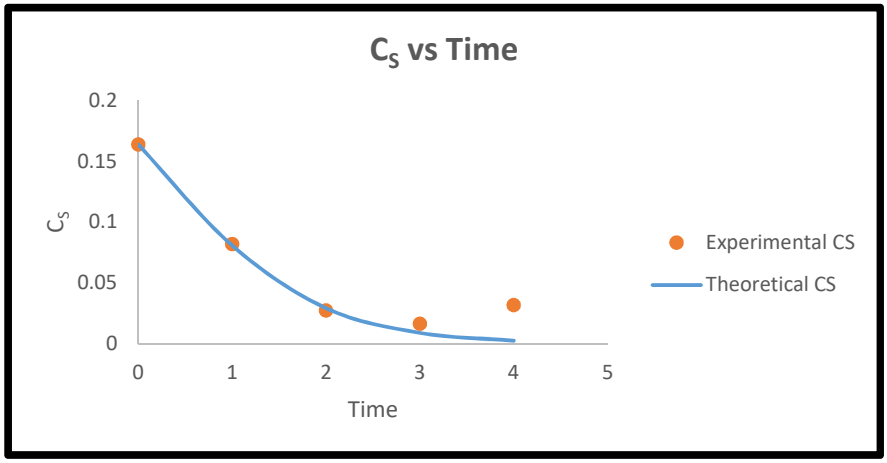

Figure 34: Theoretical and experimental substrate consumption plotted against time

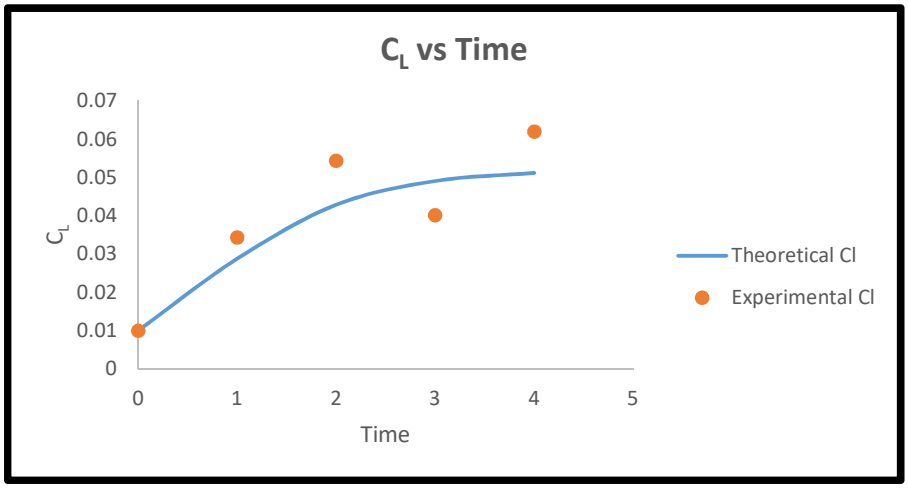

Figure 35: Theoretical and experimental lipid concentrations plotted against tim

6.7 Comparison of growth and lipid kinetics parameters in Photoautotrophic and Photo heterotrophic growth mode

According to table 9, it was found that in comparison to photoheterotrophic culture condition, the maximum specific growth rate as well as the productivity was higher in case of photoautotrophic mode of cultivation.

Table 9: Growth kinetics parameters determined in the present study in different growth modes

Parameters	Photoautotrophic	Photo heterotrophic
Highest biomass concentration (C_X)	0.7246 g/L for 15% batch on 2nd day	0.817 g/L for 15% glycerol on 4th day
Highest biomass productivity ($P_{Biomass}$)	0.2913 g/L/day for 15% batch on 2nd day	0.275799 g/L/day for 10% glycerol batch on 2nd day
Maximum specific growth rate (μ_{max})	3.667 d^{-1}	0.8826125 d^{-1}
Half saturation rate constant (K_S)	0.24972 g/L	0.01023 g/L
Inhibition constant (K_I)	0.007965 g/L	0.1945 g/L

It can be inferred, that the maximum specific growth rate in photoautotrophic mode may be due to the natural adaptation of *L. subtilis JUCHE1* to high CO_2 enriched surroundings of local thermal power plant and because of high CO2 uptake/fixation efficiency the growth rate is comparatively higher than the organic carbon (glycerol) adapted cultures in photo-heterotrophic mode of cultivation. In contrast to photoautotrophic mode, the organism has lower productivity and maximum specific growth rate in photoheterotrophic mode as the organism is adapted to grow in glycerol assisted media.

In stark contrast to the biomass concentration it can be seen that the lipid content as well as lipid productivity is significantly more in photoheterotrophic mode in comparison to photoautotrophic mode. The lipid content obtained in glycerol assisted culture is 4.5 folds of CO_2 assisted cultures. Similarly, as seen in Table 10, the lipid productivity photoheterotrophic mode is also 3 folds of lipid productivity obtained in photoautotrophic mode.

Table 10: Lipid kinetics parameters investigated in the present study in different growth modes

Parameters	Photoautotrophic	Photoheterotrophic
Highest lipid content ($L\%$)	12.499% for 15% batch on 4th day	56.345% for 5% batch on 4th day
Highest lipid productivity (P_{Lipid})	0.0219 g/L/day for 15% batch on 2nd day	0.062055 g/L/day for 15% on 4th day
Maximum specific rate of lipid formation ($q_{p_{\max}}$)	0.15289 day^{-1}	0.15701 day^{-1}
Half saturation rate constant (K_s)	0.04932 g/L	2.7 x 10^{-3} g/L
Inhibition constant (K_i)	0.0404 g/L	0.73804 g/L.

The possible explanation for this occurrence is that perhaps the organism is able to uptake glycerol more efficiently by membrane transports which is more efficient than the photosynthetic mode. Once inside the cells, the glycerol can easily enter the fatty acid synthesis cycle breaking glycerol to pyruvate to yield Malonyl CoA which ultimately leads to synthesis of Poly Unsaturated Fatty Acids (PUFA). Since glycerol accumulation may be due the effect of stressors, there is a chance that glycerol metabolism in *L. subtilis JUCHE1* is also affected by the same. By looking at data provided in Table 10, the strain shows oleaginous trait in photoheterotrophy.

Chapter 7: Conclusion

In the present study investigations have been made to determine the growth and lipid kinetics parameters of algal strain *L. subtilis JUCHE1* in photoautotrophic and photoheterotrophic growth modes. In case of lipid accumulation and productivity, the highest content was obtained for photoheterotrophic growth in comparison to the photoautotrophic mode which signifies that the strain shows oleaginous trait in photoheterotrophic mode of growth by sacrificing growth and biomass productivity. The study also identified that the algal oil extracted from the chosen strain contains essential fatty acids. Model simulation has been conducted for predicting fit of experimental and theoretical data obtained by solving the differential mass balance equations have been solved for the experiments conducted with CO_2 concentration of 15%. Furthermore, pigment extraction was undertaken in the current study that suggests that Dimethyl sulphoxide is a good solvent for extracting Chlorophyll a and b while Diethyl ether gives better results for carotenoid extraction. Further studies are necessary to be undertaken to identify the stressors affecting biomass and lipid productivities. It will be also useful to investigate the relation between growth and lipid production.

References

1. Adamczyk, M., Lasek, J., & Skawińska, A. (2016). CO 2 biofixation and growth kinetics of Chlorella vulgaris and Nannochloropsis gaditana. *Applied biochemistry and biotechnology*, *179*(7), 1248-1261.
2. Aubert, S., Gout, E., Bligny, R., & Douce, R. (1994). Multiple effects of glycerol on plant cell metabolism. Phosphorus-31 nuclear magnetic resonance studies. *Journal of Biological Chemistry*, *269*(34), 21420-21427.
3. Chen, C. Y., Chang, H. W., Kao, P. C., Pan, J. L., & Chang, J. S. (2012). Biosorption of cadmium by CO2-fixing microalga Scenedesmus obliquus CNW-N. *Bioresource technology*, *105*, 74-80.
4. Chen, F., Zhang, Y., & Guo, S. (1996). Growth and phycocyanin formation of Spirulina platensis in photoheterotrophic culture. *Biotechnology letters*, *18*(5), 603-608.
5. Chowdhury, R., Das, S., & Ghosh, S. (2018). CO 2 Capture and Utilization (CCU) in Coal-Fired Power Plants: Prospect of In Situ Algal Cultivation. In *Sustainable Energy Technology and Policies* (pp. 231-254). Springer, Singapore.
6. climatecentral.org (2019), *Rising Global Temperatures and CO_2;* Retrieved from: https://www.climatecentral.org/gallery/graphics/co2-and-rising-global-temperatures [Accessed on 20 May, 2018]
7. Concas, A., Malavasi, V., Costelli, C., Fadda, P., Pisu, M., & Cao, G. (2016). Autotrophic growth and lipid production of Chlorella sorokiniana in lab batch and BIOCOIL photobioreactors: Experiments and modeling. *Bioresource technology*, *211*, 327-338.
8. Cuellar-Bermudez, S. P., Aguilar-Hernandez, I., Cardenas-Chavez, D. L., Ornelas-Soto, N., Romero-Ogawa, M. A., & Parra-Saldivar, R. (2015). Extraction and purification of high-value metabolites from microalgae: essential lipids, astaxanthin and phycobiliproteins. *Microbial biotechnology*, *8*(2), 190-209.
9. De Morais, M. G., & Costa, J. A. V. (2007). Biofixation of carbon dioxide by Spirulina sp. and Scenedesmus obliquus cultivated in a three-stage serial tubular photobioreactor. *Journal of biotechnology*, *129*(3), 439-445.
10. de Morais, M. G., & Costa, J. A. V. (2007). Isolation and selection of microalgae from coal fired thermoelectric power plant for biofixation of carbon dioxide. *Energy Conversion and Management*, *48*(7), 2169-2173.

11. Deng, X., Li, Y., & Fei, X. (2009). Microalgae: a promising feedstock for biodiesel. *African Journal of Microbiology Research*, *3*(13), 1008-1014.
12. Drapcho, C. M., Nhuan, N. P., & Walker, T. H. (2008). *Biofuels engineering process technology* (No. Sirsi) i9780071487498). New York: McGraw-Hill.
13. Eriksen, N. T. (2008). The technology of microalgal culturing. *Biotechnology letters*, *30*(9), 1525-1536.
14. globalcarbonatlas.org (2019), CO_2 emissions, Retrieved from: http://www.globalcarbonatlas.org/en/CO2-emissions [Accessed on 29 April, 2019]
15. Gutiérrez-Arriaga, C. G., Serna-González, M., Ponce-Ortega, J. M., & El-Halwagi, M. M. (2014). Sustainable integration of algal biodiesel production with steam electric power plants for greenhouse gas mitigation. *ACS Sustainable Chemistry & Engineering*, *2*(6), 1388-1403.
16. Harmut, A. (1987). Chlorophylls and carotenoids: pigments of photosynthetic membranes. *Methods Enzymol.*, *148*, 350-383.
17. Ho, S. H., Chen, C. Y., Lee, D. J., & Chang, J. S. (2011). Perspectives on microalgal CO2-emission mitigation systems—a review. *Biotechnology advances*, *29*(2), 189-198.
18. Ho, S. H., Lu, W. B., & Chang, J. S. (2012). Photobioreactor strategies for improving the CO2 fixation efficiency of indigenous Scenedesmus obliquus CNW-N: statistical optimization of CO2 feeding, illumination, and operation mode. *Bioresource technology*, *105*, 106-113.
19. Huang, Y. T., & Su, C. P. (2014). High lipid content and productivity of microalgae cultivating under elevated carbon dioxide. *International Journal of Environmental Science and Technology*, *11*(3), 703-710.
20. ieabioenergy.com (2019), *Bi-based chemicals, value added products from biorefineries*; Retrieved from: https://www.ieabioenergy.com/wp-content/uploads/2013/10/Task-42-Biobased-Chemicals-value-added-products-from-biorefineries.pdf [Accessed on 20 April, 2019]
21. Kargi, F., & Shuler, M. L. (1992). *Bioprocess engineering: basic concepts*. Prentice-Hall PTR.
22. Kargupta, W., Ganesh, A., & Mukherji, S. (2015). Estimation of carbon dioxide sequestration potential of microalgae grown in a batch photobioreactor. *Bioresource technology*, *180*, 370-375.

23. Khanra, A., Vasistha, S., & Rai, M. P. (2017). Glycerol on lipid enhancement and fame characterization in algae for raw material of biodiesel. *International Journal of Renewable Energy Research (IJRER)*, *7*(4), 1970-1978.
24. Klinthong, W., Yang, Y. H., Huang, C. H., & Tan, C. S. (2015). A review: microalgae and their applications in CO2 capture and renewable energy. *Aerosol Air Qual Res*, *15*(2), 712-742.
25. Kong, W. B., Yang, H., Cao, Y. T., Song, H., Hua, S. F., & Xia, C. G. (2013). Effect of glycerol and glucose on the enhancement of biomass, lipid and soluble carbohydrate production by Chlorella vulgaris in mixotrophic culture. *Food Technol Biotechnol*, *51*(1), 62-69.
26. Kumar, K., & Das, D. (2012). Growth characteristics of Chlorella sorokiniana in airlift and bubble column photobioreactors. *Bioresource technology*, *116*, 307-313.
27. Kundu, A., Basu, J. K., & Das, G. (2012). A novel gas–liquid contactor for chemisorption of CO2. *Separation and purification technology*, *94*, 115-123.
28. Leite, G. B., Paranjape, K., Abdelaziz, A. E., & Hallenbeck, P. C. (2015). Utilization of biodiesel-derived glycerol or xylose for increased growth and lipid production by indigenous microalgae. *Bioresource technology*, *184*, 123-130.
29. Lin, H., Fang, L., Low, C. S., Chow, Y., & Lee, Y. K. (2013). Occurrence of glycerol uptake in Dunaliella tertiolecta under hyperosmotic stress. *The FEBS journal*, *280*(4), 1064-1072.
30. lpi.oregonstate.edu (2018), *Essential fatty acids*; Retrieved from: https://lpi.oregonstate.edu/book/export/html/362 [Accessed on 25 May, 2019]
31. Mandotra, S. K., Kumar, P., Suseela, M. R., & Ramteke, P. W. (2014). Fresh water green microalga Scenedesmus abundans: a potential feedstock for high quality biodiesel production. *Bioresource technology*, *156*, 42-47.
32. Mejia Rendon, S. (2014). Effects of Light, Co2 and Reactor Design on Growth of Algae: An Experimental Approach to Increase Biomass Production.
33. Minhas, A. K., Hodgson, P., Barrow, C. J., & Adholeya, A. (2016). A review on the assessment of stress conditions for simultaneous production of microalgal lipids and carotenoids. *Frontiers in microbiology*, *7*, 546.
34. Murakami, M., Yamada, F., Nishide, T., Muranaka, T., Yamaguchi, N., & Takimoto, Y. (1998). The biological CO2 fixation using Chlorella sp. with high capability in fixing CO2. In *Studies in Surface Science and Catalysis* (Vol. 114, pp. 315-320). Elsevier.

35. Nelson, D. L., Lehninger, A. L., & Cox, M. M. (2008). *Lehninger principles of biochemistry*. Macmillan.
36. Pegallapati, A. K., & Nirmalakhandan, N. (2013). Internally illuminated photobioreactor for algal cultivation under carbon dioxide-supplementation: Performance evaluation. *Renewable energy*, *56*, 129-135.
37. Perez-Garcia, O., Escalante, F. M., de-Bashan, L. E., & Bashan, Y. (2011). Heterotrophic cultures of microalgae: metabolism and potential products. *Water research*, *45*(1), 11-36.
38. Pires, J. C. M., Alvim-Ferraz, M. C. M., Martins, F. G., & Simões, M. (2012). Carbon dioxide capture from flue gases using microalgae: engineering aspects and biorefinery concept. *Renewable and sustainable energy reviews*, *16*(5), 3043-3053.
39. Pokoo-Aikins, G., Nadim, A., El-Halwagi, M. M., & Mahalec, V. (2010). Design and analysis of biodiesel production from algae grown through carbon sequestration. *Clean Technologies and Environmental Policy*, *12*(3), 239-254.
40. Porra, R. J., Thompson, W. A., & Kriedemann, P. E. (1989). Determination of accurate extinction coefficients and simultaneous equations for assaying chlorophylls a and b extracted with four different solvents: verification of the concentration of chlorophyll standards by atomic absorption spectroscopy. *Biochimica et Biophysica Acta (BBA)-Bioenergetics*, *975*(3), 384-394.
41. Pradhan, L. (2014). *Studies on Carbon Sequestration through Microalgal Culture in Photobioreactor* (Doctoral dissertation).
42. Pradhan, L., Bhattacharjee, V., Mitra, R., Bhattacharya, I., & Chowdhury, R. (2015). Biosequestration of CO2 using power plant algae (Rhizoclonium hieroglyphicum JUCHE2) in a Flat Plate Photobio-Bubble-Reactor–Experimental and modeling. *Chemical Engineering Journal*, *275*, 381-390.
43. Pruvost, J., Van Vooren, G., Cogne, G., & Legrand, J. (2009). Investigation of biomass and lipids production with Neochloris oleoabundans in photobioreactor. *Bioresource technology*, *100*(23), 5988-5995.
44. Pruvost, J., Van Vooren, G., Le Gouic, B., Couzinet-Mossion, A., & Legrand, J. (2011). Systematic investigation of biomass and lipid productivity by microalgae in photobioreactors for biodiesel application. *Bioresource technology*, *102*(1), 150-158.
45. Razzak, S. A., Ilyas, M., & Hossain, M. M. Effect of Different Ratio of Air-CO2 Mixing Feed on the Growth of Chlorella Vulgaris and Nannochloropsis Oculata in

Batch Photobioreactors.

46. Ren, H., Tuo, J., Addy, M. M., Zhang, R., Lu, Q., Anderson, E., ... & Ruan, R. (2017). Cultivation of Chlorella vulgaris in a pilot-scale photobioreactor using real centrate wastewater with waste glycerol for improving microalgae biomass production and wastewater nutrients removal. *Bioresource technology*, *245*, 1130-1138.
47. Richmond, A., & Hu, Q. (2013). *Handbook of microalgal culture: applied phycology and biotechnology*. John Wiley & Sons.
48. Robaina, R. R., Garcia-Jimenez, P., Brito, I., & Luque, A. (1995). Light control of the respiration of exogenous glycerol in the red macroalga Grateloupia doryphora. *European Journal of Phycology*, *30*(2), 81-86.
49. Salih, F. M. (2011). Microalgae tolerance to high concentrations of carbon dioxide: a review. *Journal of Environmental Protection*, *2*(05), 648.
50. Sander, R. (2015). Compilation of Henry's law constants (version 4.0) for water as solvent. *Atmospheric Chemistry & Physics*, *15*(8).
51. shrinkthatfootprint.com (2018), *Burning the Carbon Sink;* Retrieved from: http://shrinkthatfootprint.com/burning-the-carbon-sink [Accessed on 15 May, 2019]
52. Sumanta, N., Haque, C. I., Nishika, J., & Suprakash, R. (2014). Spectrophotometric analysis of chlorophylls and carotenoids from commonly grown fern species by using various extracting solvents. *Res J Chem Sci*, *2231*, 606X.
53. Vonshak, A., Cheung, S. M., & Chen, F. (2000). Mixotrophic growth modifies the response of Spirulina (Arthrospira) platensis (Cyanobacteria) cells to light. *Journal of Phycology*, *36*(4), 675-679.
54. Vunjak-Novakovic, G., Kim, Y., Wu, X., Berzin, I., & Merchuk, J. C. (2005). Air-lift bioreactors for algal growth on flue gas: mathematical modeling and pilot-plant studies. *Industrial & engineering chemistry research*, *44*(16), 6154-6163.
55. Wang, B., Li, Y., Wu, N., & Lan, C. Q. (2008). CO 2 bio-mitigation using microalgae. *Applied microbiology and biotechnology*, *79*(5), 707-718.
56. Wang, Z., Wen, X., Xu, Y., Ding, Y., Geng, Y., & Li, Y. (2018). Maximizing CO2 biofixation and lipid productivity of oleaginous microalga Graesiella sp. WBG1 via CO2-regulated pH in indoor and outdoor open reactors. *Science of the Total Environment*, *619*, 827-833.
57. Zeng, X., Danquah, M. K., Chen, X. D., & Lu, Y. (2011). Microalgae bioengineering: from CO2 fixation to biofuel production. *Renewable and Sustainable Energy*

Reviews, *15*(6), 3252-3260.